



Article

# Altered GABA<sub>A</sub> Receptor Expression in the Primary Somatosensory Cortex of a Mouse Model of Genetic Absence Epilepsy

Muhammad Hassan, Nadia K. Adotevi and Beulah Leitch \*

Department of Anatomy, School of Biomedical Sciences, and the Brain Health Research Centre, University of Otago, P.O. Box 913, Dunedin 9054, New Zealand

\* Correspondence: beulah.leitch@otago.ac.nz; Tel.: +64-3-479-7618

**Abstract:** Absence seizures are hyperexcitations within the cortico-thalamocortical (CTC) network, however the underlying causative mechanisms at the cellular and molecular level are still being elucidated and appear to be multifactorial. Dysfunctional feed-forward inhibition (FFI) is implicated as one cause of absence seizures. Previously, we reported altered excitation onto parvalbumin-positive (PV<sup>+</sup>) interneurons in the CTC network of the stargazer mouse model of absence epilepsy. In addition, downstream changes in GABAergic neurotransmission have also been identified in this model. Our current study assessed whether dysfunctional FFI affects GABA<sub>A</sub> receptor (GABA<sub>A</sub>R) subunit expression in the stargazer primary somatosensory cortex (SoCx). Global tissue expression of GABA<sub>A</sub>R subunits  $\alpha$ 1,  $\alpha$ 3,  $\alpha$ 4,  $\alpha$ 5,  $\beta$ 2,  $\beta$ 3,  $\gamma$ 2 and  $\delta$  were assessed using Western blotting (WB), while biochemically isolated subcellular fractions were assessed for the  $\alpha$  and  $\delta$  subunits. We found significant reductions in tissue and synaptic expression of GABA<sub>A</sub>R  $\alpha$ 1, 18% and 12.2%, respectively. However, immunogold-cytochemistry electron microscopy (ICC-EM), conducted to assess GABA<sub>A</sub>R  $\alpha$ 1 specifically at synapses between PV<sup>+</sup> interneurons and their targets, showed no significant difference. These data demonstrate a loss of phasic GABA<sub>A</sub>R  $\alpha$ 1, indicating altered GABAergic inhibition which, coupled with dysfunctional FFI, could be one mechanism contributing to the generation or maintenance of absence seizures.

**Keywords:** GABA<sub>A</sub> receptors; absence epilepsy; stargazer mouse; Western blotting; biochemical fractionation; immunogold-cytochemistry electron microscopy; cortico-thalamocortical network; primary somatosensory cortex



**Citation:** Hassan, M.; Adotevi, N.K.; Leitch, B. Altered GABA<sub>A</sub> Receptor Expression in the Primary Somatosensory Cortex of a Mouse Model of Genetic Absence Epilepsy.

*Int. J. Mol. Sci.* **2022**, *23*, 15685.  
<https://doi.org/10.3390/ijms232415685>

Academic Editor: Aurel Popa-Wagner

Received: 9 November 2022  
Accepted: 7 December 2022  
Published: 10 December 2022

**Publisher's Note:** MDPI stays neutral with regard to jurisdictional claims in published maps and institutional affiliations.



**Copyright:** © 2022 by the authors. Licensee MDPI, Basel, Switzerland. This article is an open access article distributed under the terms and conditions of the Creative Commons Attribution (CC BY) license (<https://creativecommons.org/licenses/by/4.0/>).

## 1. Introduction

Childhood absence epilepsy is a complex genetic neurological disorder characterized by generalized absence seizures, detected on electroencephalography (EEG) as hallmark 2.5–4 Hz spike-wave discharges (SWDs) [1,2]. It is a common pediatric syndrome accounting for nearly 10–17% of all childhood epilepsies [3]. SWDs are associated with hyperexcitations in the brain's CTC network, which comprises reciprocal excitatory connections between the cortex and relay thalamus modulated by FFI PV<sup>+</sup> inhibitory interneurons within the reticular thalamic nucleus (RTN) thalamus and cortex [1,4]. Pathological hyperexcitations can arise from disruptions in cellular and molecular activity within the CTC microcircuit network through multiple mechanisms. One such implicated mechanism involves impaired GABA<sub>A</sub>R expression caused by mutations in GABA<sub>A</sub>R subunit genes, such as in the  $\alpha$ 1 subunit gene [5,6] and R43Q mutation in the  $\gamma$ 2 gene [7–10] observed in human patients. Significantly, the induction of these gene mutations in rodent models caused SWDs associated with altered GABA<sub>A</sub>R subunit expression and altered inhibition in the CTC network [11–15]. Although in some genetic absence seizure rodent models, such as the stargazer mouse, the primary genetic defect is not present in the GABA<sub>A</sub>Rs,

these models often display secondary GABAergic changes thought to play a significant role in the generation or maintenance of SWDs [16].

The stargazer mouse presents with a primary genetic defect resulting in a deficit of stargazin [17,18], and we have previously demonstrated that this leads to a deficit of glutamatergic GluA4-containing  $\alpha$ -amino-3-hydroxy-5-methyl-4-isoxazolepropionic acid (AMPA) receptors at excitatory synapses on PV<sup>+</sup> feed-forward inhibitory interneurons of RTN [19], and primary SoCx [20–22]. Within the CTC network, activation of PV<sup>+</sup> interneurons by cortical glutamatergic inputs at RTN manifests as FFI of thalamocortical relay neurons. Similarly, in the primary SoCx, activation of these interneurons by glutamatergic inputs from thalamocortical relay neurons leads to FFI of target principal neurons. Hence, seizure generation in the stargazer mouse model may be mediated by dysfunctional FFI, secondary to loss of AMPA receptors at PV<sup>+</sup> interneurons, leading to disinhibition in the CTC network. This has been corroborated by our recent findings, where silencing PV<sup>+</sup> interneurons in both the RTN and primary SoCx of mice, using Designer Receptors Exclusively Activated by Designer Drugs (DREADD) technology, induced absence-like SWDs [23], while activating them abolished pharmacologically induced SWDs [24].

The stargazin mutation is also associated with downstream changes in GABA<sub>A</sub>R subunit expression in multiple brain regions [25–27]. In the stargazer ventroposterior (VP) thalamic nucleus, we previously reported a specific increase in both tonic and phasic GABA<sub>A</sub>R subunits [28,29]. However, unlike the AMPA receptor loss, which is pre-seizure, the increase in GABA<sub>A</sub>R subunits expression in the thalamus occurs after the onset of seizures [30], and thus is unlikely to be causative of seizures, although a role in seizure maintenance should not be ruled out. GABA<sub>A</sub>Rs generate either phasic or tonic post-inhibitory currents depending on synaptic or extra-synaptic GABAergic activation, respectively [31]. Evidence suggests a variable change in phasic inhibition and increased tonic inhibition to be involved based on the animal model as well as the region of the CTC network observed [32]. Enhanced tonic inhibition in the VP thalamic relay nucleus due to GAT-1 malfunction has been identified as a potential source of SWDs [33,34]. However, this increase is detectable at varying periods in the different models and cannot be positively pinpointed as a cause or effect of the SWDs. The cortex has been suggested as the principal initiation site of the SWDs, with the initiation site focused on deep layers of the primary SoCx of rodent models [35–38]. Cortical initiation of seizures is also supported by EEG, magnetoencephalography (MEG), and functional magnetic resonance imaging evidence from human patients [1]. However, in the stargazer primary SoCx, GABA<sub>A</sub>R expression and function, which may have a role in the mechanisms of absence seizures, have not yet been investigated.

The rodent neocortex expresses GABA<sub>A</sub>R subunits  $\alpha$ 1– $\alpha$ 5,  $\beta$ 1– $\beta$ 3,  $\gamma$ 2– $\gamma$ 3, and  $\delta$  [39], with the subunit combination of synaptic  $\alpha$ 1 $\beta$ 2 $\gamma$ 2 by far the most abundantly expressed [40,41]. The principal mediator of potent and rapid inhibitory currents is the  $\alpha$ 1-containing phasic GABA<sub>A</sub>R [31,42,43], which is ubiquitously expressed in the cortex [44], with preferentially peri-somatic and peripheral dendritic expression on pyramidal neurons. These sites on pyramidal neurons are also convergence points for connectivity from fast-spiking PV<sup>+</sup> interneurons [45]. To test our hypothesis that dysfunctional PV<sup>+</sup> interneurons-mediated FFI could alter  $\alpha$ 1-containing synaptic GABA<sub>A</sub>R expression on target neurons to promote the initiation or maintenance of SWDs, we conducted a series of experiments, predominantly addressing changes in the ubiquitous GABA<sub>A</sub>R  $\alpha$ 1 subunit. Other relevant GABA<sub>A</sub>R subunits were also assessed for any concomitant changes. Collateral changes in subunits  $\alpha$ 3,  $\beta$ 2,  $\beta$ 3, and  $\gamma$ 2 have been reported in other mouse models where the phasic GABA<sub>A</sub>R  $\alpha$ 1 subunit was compromised [12,13,46]. Since altered tonic inhibition has also been implicated in the generation of SWDs [34,47], stargazer primary SoCx was also probed for the  $\alpha$ 4,  $\alpha$ 5, and  $\delta$  subunits, found predominantly in GABA<sub>A</sub>Rs mediating tonic inhibition [31]. Immunofluorescence confocal microscopy was conducted to confirm the cortical layer-specific distribution and PV<sup>+</sup> cellular localization of GABA<sub>A</sub>R  $\alpha$ 1 in the primary SoCx of the homozygous epileptic (E, stg/stg) stargazers compared to

control non-epileptic (NE; heterozygous [+ / stg] and wild-type [+ / +]) littermates. Semi-quantitative WB analysis of whole primary SoCx was used to investigate tissue changes in GABA<sub>A</sub>R subunits  $\alpha 1$ ,  $\alpha 3$ ,  $\alpha 4$ ,  $\alpha 5$ ,  $\beta 2$ ,  $\beta 3$ ,  $\gamma 2$ , and  $\delta$ . Biochemical fractionation was then used to isolate synaptic and extra-synaptic fractions from the primary SoCx, which were subsequently probed for GABA<sub>A</sub>R subunits  $\alpha 1$ ,  $\alpha 3$ ,  $\alpha 4$ ,  $\alpha 5$ , and  $\delta$ . Finally, double-labelled ICC-EM was used to quantify relative levels of GABA<sub>A</sub>R  $\alpha 1$  at synapses between PV<sup>+</sup> interneurons and their targets in primary SoCx.

## 2. Results

### 2.1. GABA<sub>A</sub>R $\alpha 1$ Is Expressed in all Primary SoCx Layers

Confocal immunofluorescence (Figure 1A–C) confirmed the presence of GABA<sub>A</sub>R  $\alpha 1$  in all layers of the primary SoCx in the control littermates and stargazers (Figure 1A). GABA<sub>A</sub>R  $\alpha 1$  immunofluorescence displayed nearly uniform distribution across cortical layers, with relatively higher intensity in layer IV, identified by labelling with VGlut2 (Figure 1C), which intensely labels excitatory thalamocortical terminals projecting to cortical layer IV [48–51]. This distribution pattern of GABA<sub>A</sub>R  $\alpha 1$  across cortical layers has been reported previously [39,52]. PV<sup>+</sup> somas were seen in all layers except layer 1 (Figure 1B), as previously reported [53–55]. Higher numbers were apparent in layers IV and V, which concurs with our previously published report [21]. Figure 2 shows merged images for PV and GABA<sub>A</sub>R  $\alpha 1$ , demonstrating co-labelling of GABA<sub>A</sub>R  $\alpha 1$  and PV<sup>+</sup> in PV<sup>+</sup> somas as well as the surrounding neuropil, which agrees with published reports [56]. Both GABA<sub>A</sub>R  $\alpha 1$  pre-adsorption and omission controls showed virtually no fluorescence (Supplementary Figure S1), which confirmed the specificity of the GABA<sub>A</sub>R  $\alpha 1$  antibody.

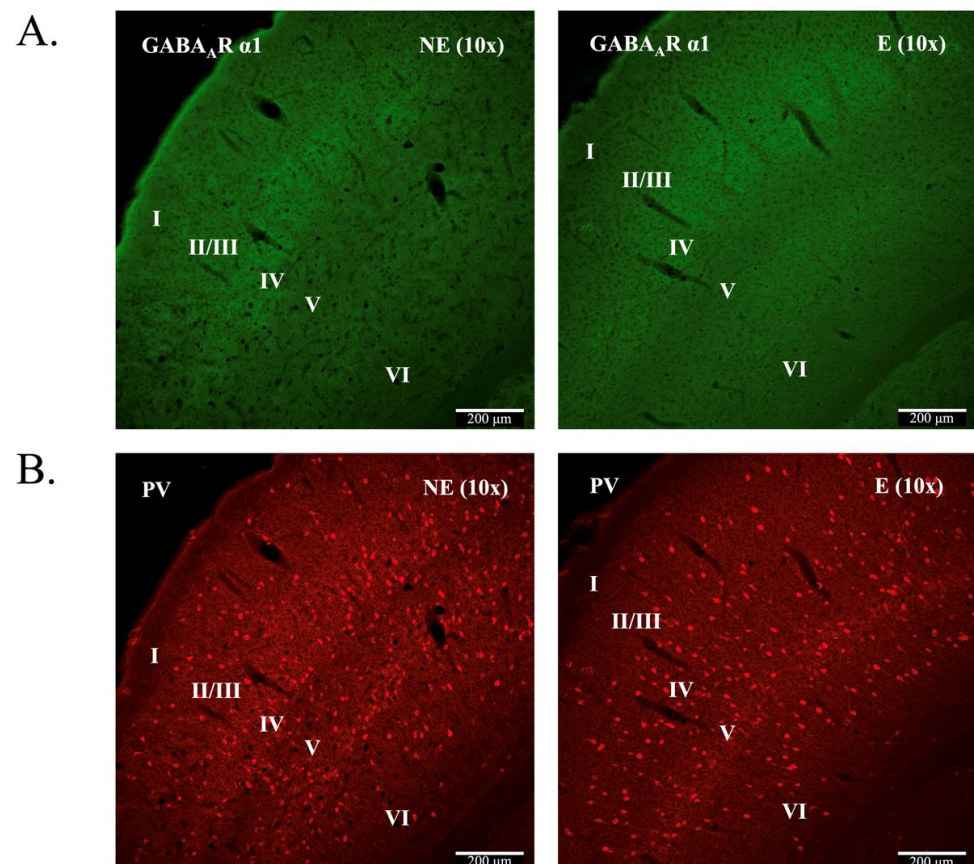
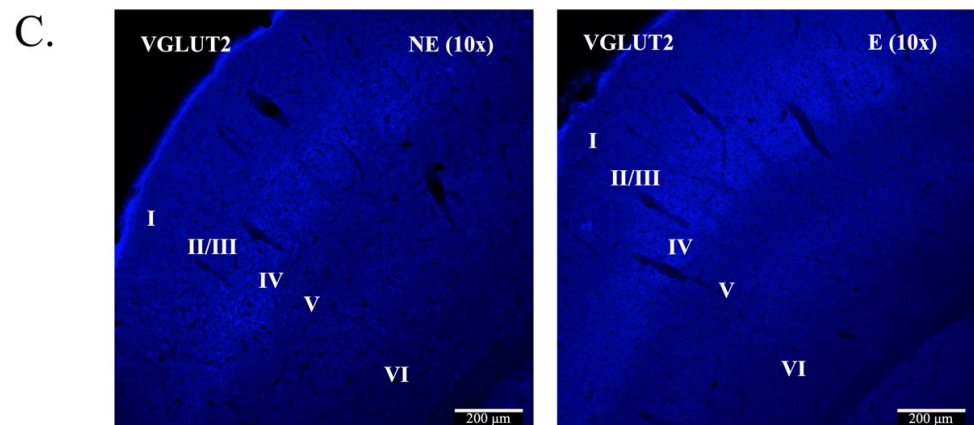
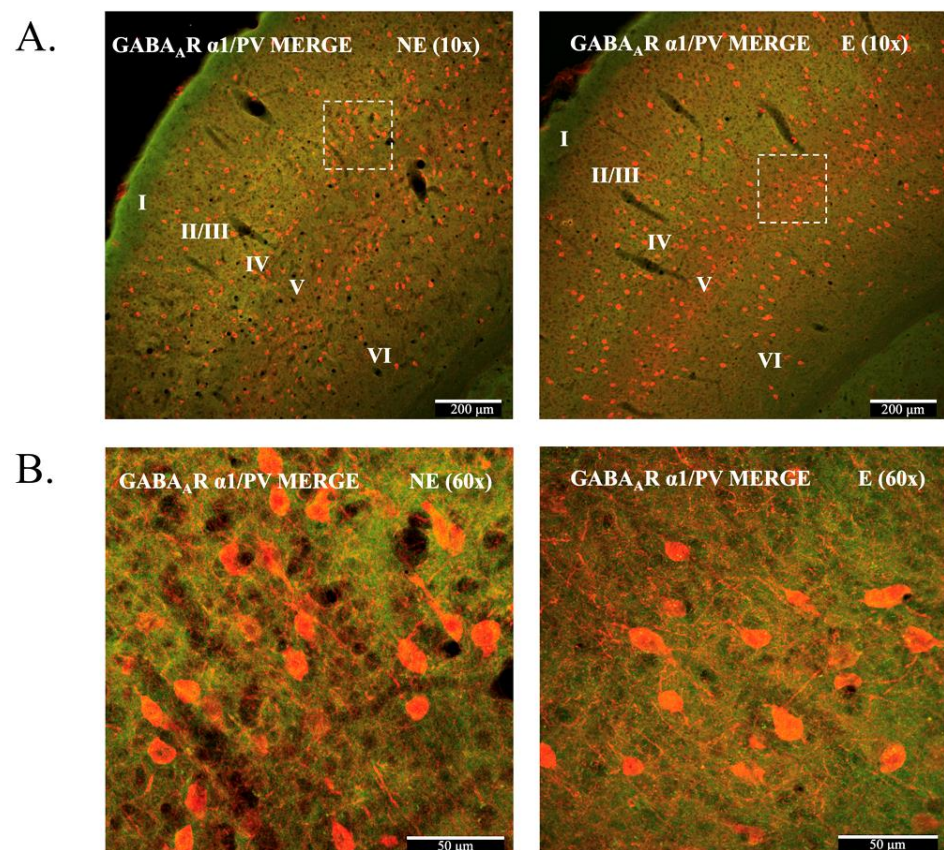


Figure 1. Cont.



**Figure 1.** Representative confocal immunofluorescence images demonstrating expression of GABA<sub>A</sub>R  $\alpha$ 1 in the stargazer primary SoCx. 10 $\times$  (Objective: 10 $\times$  Plan) magnification from control (NE) littermate and epileptic (E) stargazer are shown here. (A) Pseudo-green channel shows diffuse labelling for GABA<sub>A</sub>R  $\alpha$ 1 subunit across the cortical layers with higher intensity in layer IV. (B) Pseudo-red channel shows labelling for PV<sup>+</sup> neurons. The soma of PV<sup>+</sup> neurons are present in all layers except layer I. (C) Pseudo-blue channel shows VGLut2 which assists in identification of the cortical layers. Intense labelling can be seen, predominantly, in layer IV due to the presence of thalamocortical excitatory nerve terminals.



**Figure 2.** Merged confocal immunofluorescence images demonstrating the co-localisation for GABA<sub>A</sub>R  $\alpha$ 1 and PV in the primary SoCx of control (NE) littermate and epileptic (E) stargazer. (A) 10 $\times$  magnification of GABA<sub>A</sub>R  $\alpha$ 1/PV merged image shows co-localisation of GABA<sub>A</sub>R  $\alpha$ 1 with PV<sup>+</sup> somas and processes. (B) 60 $\times$  (Objective: 60 $\times$  PlanApo oil) magnification of GABA<sub>A</sub>R  $\alpha$ 1/PV merged image clearly shows GABA<sub>A</sub>R  $\alpha$ 1 present throughout the cortex as well on PV somas.

## 2.2. Reduced GABA<sub>A</sub>R α1 Levels in the Stargazer Primary SoCx with no Change Seen in Other Subunits

Expression levels of GABA<sub>A</sub>R α1 subunit were compared in the stargazer primary SoCx and their control NE littermates using semi-quantitative WB analysis. WB scans revealed bands at the expected molecular weights of ~50 kDa for GABA<sub>A</sub>R α1 and ~42 kDa for β-actin as recognized from the protein ladder (Figure 3A). The band intensities for GABA<sub>A</sub>R α1 were normalized against β-actin intensities. The results indicated a significant reduction of 18% in the tissue expression levels of GABA<sub>A</sub>R α1 (NE:  $0.960 \pm 0.066$  [ $n = 18$ ], E:  $0.78 \pm 0.046$  [ $n = 14$ ],  $p = 0.041$ ) in the primary SoCx of the stargazers compared to their NE littermates (Figure 3A). GABA<sub>A</sub>R α3 levels, which have been reported to show a compensatory increase in response to loss of GABA<sub>A</sub>R α1 [12,46], were not significantly different (NE:  $1.000 \pm 0.036$  [ $n = 17$ ], E:  $0.935 \pm 0.049$  [ $n = 15$ ],  $p = 0.519$ ) in stargazers compared to control littermates (Figure 3B).

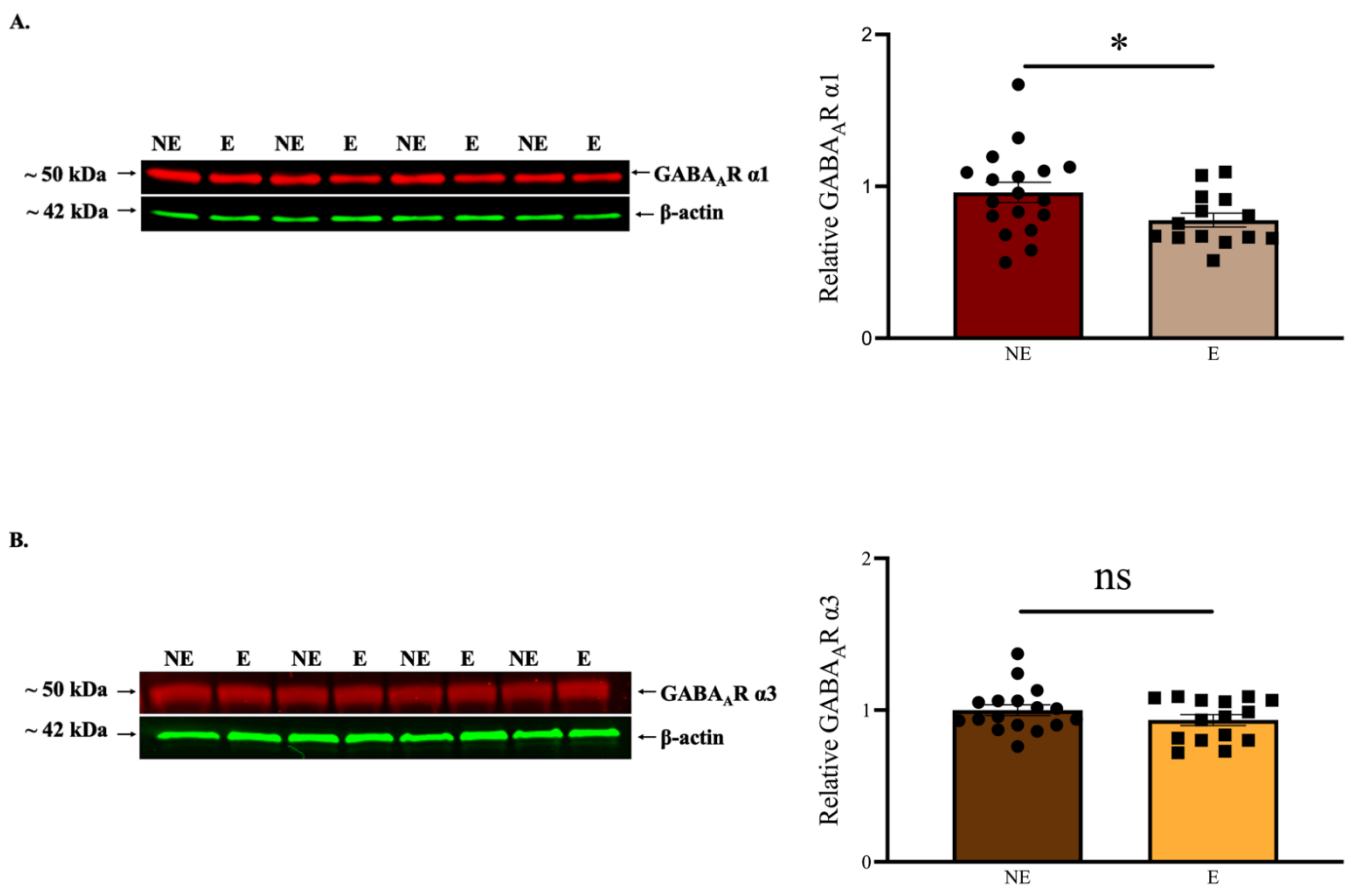


**Figure 3.** WB analysis for GABA<sub>A</sub>R α1 and α3 subunits in the primary SoCx. Data compare expression between control (NE) littermates and epileptic (E) stargazers. **(A)** Representative blots display GABA<sub>A</sub>R α1 in the primary SoCx with β-actin as the loading control. Bar graphs represent the relative expression levels of GABA<sub>A</sub>R α1 (mean ± SEM). WB analysis revealed a statistically significant reduction in whole-tissue expression levels of GABA<sub>A</sub>R α1 in the primary SoCx of the stargazers (NE:  $0.960 \pm 0.066$  [ $n = 18$ ], E:  $0.78 \pm 0.046$  [ $n = 14$ ],  $p = 0.041$ ); **(B)** Representative blots display GABA<sub>A</sub>R α3 in the primary SoCx with β-actin as the loading control. Bar graphs represent the relative expression levels of GABA<sub>A</sub>R α3. There was no statistically significant change in whole-tissue expression levels of GABA<sub>A</sub>R α3 in the primary SoCx of the stargazers (NE:  $1.000 \pm 0.036$  [ $n = 17$ ], E:  $0.935 \pm 0.049$  [ $n = 15$ ],  $p = 0.519$ ). The significance threshold was set at 0.05 with \* indicating  $p < 0.05$ . 'ns' indicates no significant change found from analyses.

GABA<sub>A</sub>R  $\beta$ 2,  $\beta$ 3 and  $\gamma$ 2 subunits are required for the arrangement of a functional pentameric  $\alpha$ 1-containing phasic GABA<sub>A</sub>R [57,58]. In addition, these subunits are also functionally expressed in tonic GABA<sub>A</sub>R combinations. Reduced expression of GABA<sub>A</sub>R  $\alpha$ 1 in knock-out models of absence seizures is accompanied by concurrent changes in these subunits as well [12,46]. However, in the current study semi-quantitative WB analysis of whole-tissue lysate did not reveal any significant changes in the levels of  $\beta$ 2 (NE:  $0.917 \pm 0.091$  [ $n = 12$ ], E:  $0.678 \pm 0.050$  [ $n = 10$ ];  $p = 0.093$ ),  $\beta$ 3 (NE:  $1.000 \pm 0.067$  [ $n = 12$ ], E:  $1.070 \pm 0.109$  [ $n = 10$ ];  $p = 0.859$ ) and  $\gamma$ 2 (NE:  $1.000 \pm 0.159$  [ $n = 9$ ], E:  $0.946 \pm 0.079$  [ $n = 7$ ];  $p = 0.900$ ) subunits in the stargazers compared to their NE littermates (Figure 4A–C).

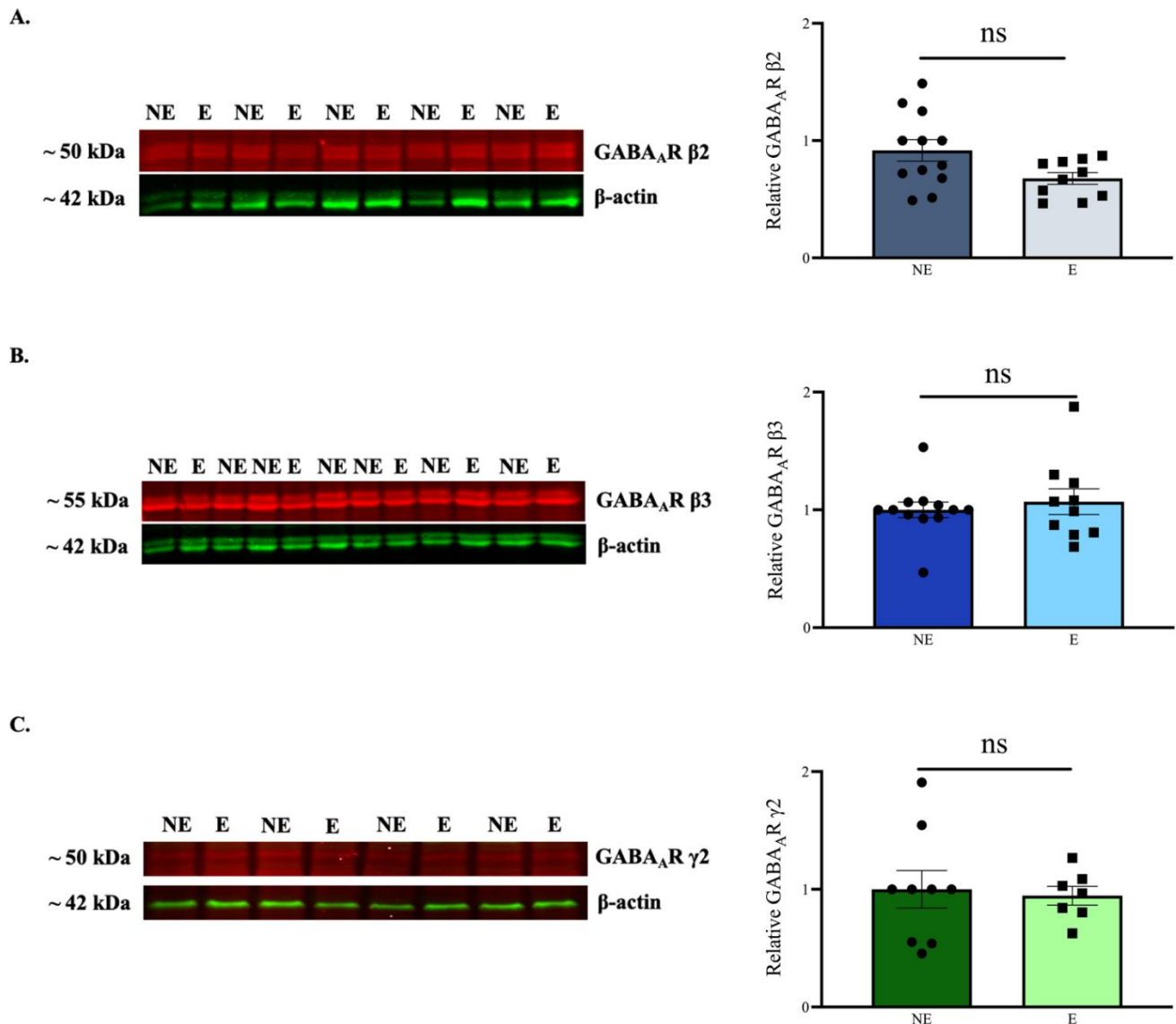


**Figure 4.** WB analysis for GABA<sub>A</sub>R  $\beta$ 2,  $\beta$ 3, and  $\gamma$ 2 subunits in the primary SoCx. The data compare expression between control (NE) littermates and epileptic (E) stargazers. (A–C) Representative blots display tissue expression of GABA<sub>A</sub>R  $\beta$ 2,  $\beta$ 3, and  $\gamma$ 2 subunits in the primary SoCx with  $\beta$ -actin as the loading control. Bar graphs represent the relative expression levels of GABA<sub>A</sub>R  $\beta$ 2,  $\beta$ 3, and  $\gamma$ 2 subunits, respectively. Bar graphs show a lack of statistically significant change in whole-tissue primary SoCx expression levels for  $\beta$ 2 (NE:  $0.917 \pm 0.091$  [ $n = 12$ ], E:  $0.678 \pm 0.050$  [ $n = 10$ ];  $p = 0.093$ ),  $\beta$ 3 (NE:  $1.000 \pm 0.067$  [ $n = 12$ ], E:  $1.070 \pm 0.109$  [ $n = 10$ ];  $p = 0.859$ ), and  $\gamma$ 2 (NE:  $1.000 \pm 0.159$  [ $n = 9$ ], E:  $0.946 \pm 0.079$  [ $n = 7$ ];  $p = 0.900$ ). The significance threshold was set at 0.05. ‘ns’ indicates no significant change found from analyses.

A recent report described the suppression of SWDs in the stargazers after an effective knock-out of GABA<sub>A</sub>R  $\delta$  subunit [47], which is expressed in GABA<sub>A</sub>Rs that mediate tonic inhibition [31]. Abnormal tonic inhibition in the stargazer VP thalamic nucleus has previously been reported [34]. Moreover, we also reported an increase in tonic GABA<sub>A</sub>R subunits  $\alpha$ 4 and  $\delta$  levels in the VP thalamic nucleus, but only after the onset of seizures in the stargazers [28,30]. To assess whether any changes in tonic GABA<sub>A</sub>R subunits occur in the adult stargazer primary SoCx, we conducted further semiquantitative WB analyses to investigate levels of GABA<sub>A</sub>R  $\alpha$ 4,  $\alpha$ 5, and  $\delta$  subunits. No significant changes in  $\alpha$ 4 (NE:  $1.000 \pm 0.063$  [ $n = 18$ ], E:  $1.117 \pm 0.095$  [ $n = 15$ ];  $p = 0.325$ ),  $\alpha$ 5 (NE:  $1.000 \pm 0.048$  [ $n = 23$ ], E:  $0.937 \pm 0.083$  [ $n = 13$ ];  $p = 0.672$ ), or  $\delta$  (NE:  $1.000 \pm 0.041$  [ $n = 27$ ], E:  $0.899 \pm 0.069$  [ $n = 23$ ];  $p = 0.215$ ) subunits were seen in the stargazer primary SoCx compared to the control littermates (Figure 5A–C).

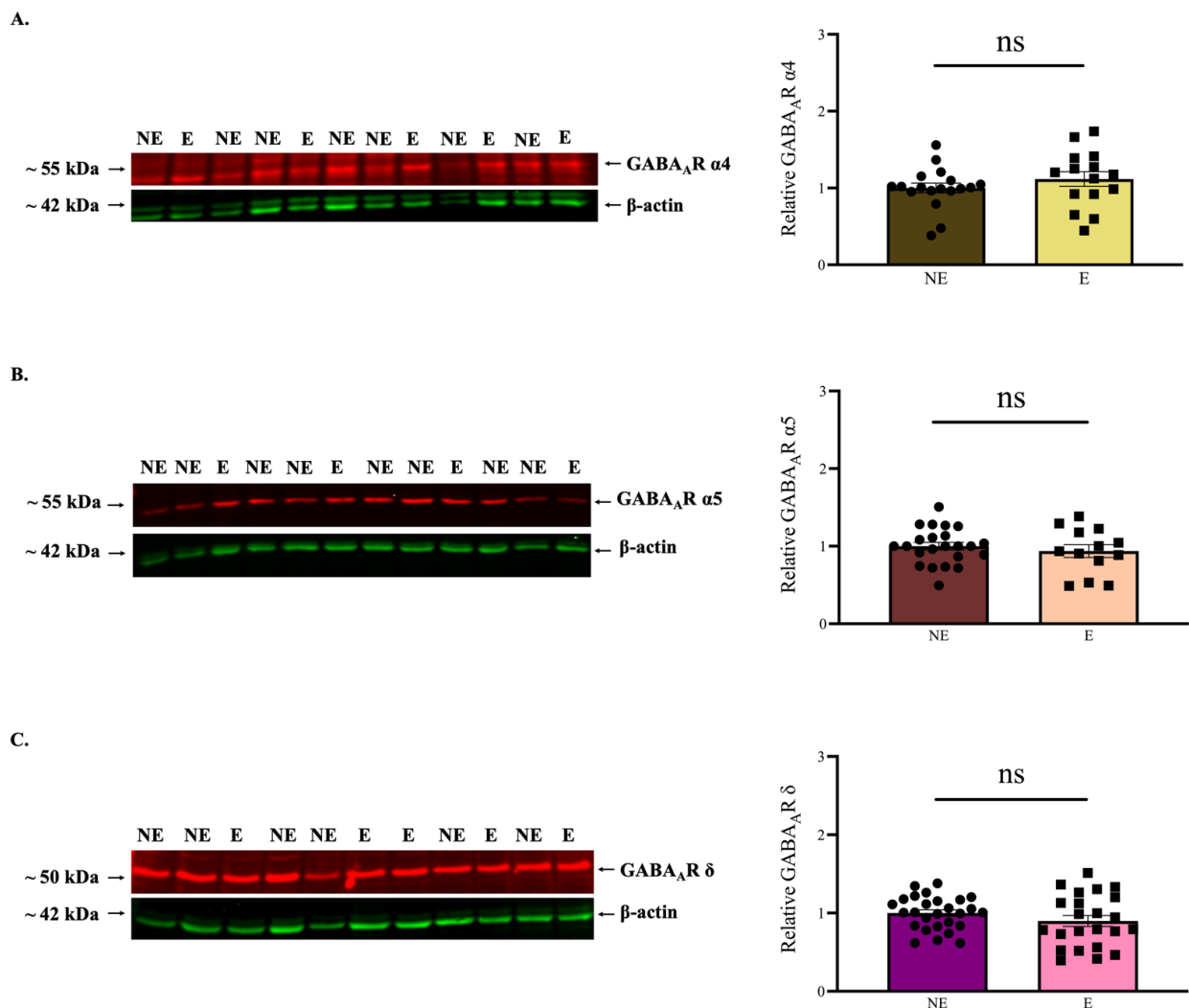


**Figure 5.** WB analysis for the principal tonic GABA<sub>A</sub>R  $\alpha$ 4,  $\alpha$ 5, and  $\delta$  subunits. Analysis compares the primary SoCx of control (NE) littermates and the epileptic (E) stargazers. (A–C) Representative blots display tissue expression of GABA<sub>A</sub>R  $\alpha$ 4,  $\alpha$ 5, and  $\delta$  subunits in the primary SoCx with  $\beta$ -actin as the loading control. Bar graphs represent the relative expression levels of GABA<sub>A</sub>R  $\alpha$ 4,  $\alpha$ 5 and  $\delta$  subunits, respectively. Bar graphs reveal a lack of statistically significant change in whole-tissue primary SoCx expression levels for GABA<sub>A</sub>R  $\alpha$ 4 (NE:  $1.000 \pm 0.063$  [ $n = 18$ ], E:  $1.117 \pm 0.095$  [ $n = 15$ ];  $p = 0.325$ ),  $\alpha$ 5 (NE:  $1.000 \pm 0.048$  [ $n = 23$ ], E:  $0.937 \pm 0.083$  [ $n = 13$ ];  $p = 0.672$ ), and  $\delta$  (NE:  $1.000 \pm 0.041$  [ $n = 27$ ], E:  $0.899 \pm 0.069$  [ $n = 23$ ];  $p = 0.215$ ). The significance threshold was set at 0.05. ‘ns’ indicates no significant change found from analyses.

### 2.3. Verification of the Biochemical Fractionation Technique

A pilot study was first conducted to validate the purity of the biochemically fractionated subcellular components. Figure 6 shows a representative Western blot of the four subcellular fractions with immunofluorescence bands detected at the specified molecular weights of 130 kDa for PanC, 95 kDa for PSD95, 50 kDa for GABA<sub>A</sub>R α1, and 42 kDa for β-actin. PanC was detected in all fractions as expected [59], whereas PSD95, a synaptic scaffold protein [20,60,61], was only present in the synaptic component and not in the extra-synaptic fraction, thus confirming the purity of the synaptic fraction. Signal values for the subunits were normalized against Pan-C, as this protein is not associated with the primary mutation in the stargazers and has been shown to remain unchanged across subcellular fractions compared to their control littermates [20,62,63]. β-actin showed variable enrichment in the four synaptic components and was not used as a normalization protein in this instance due to its inconsistent expression and association with membranous components [20,62,64]. As expected, GABA<sub>A</sub>R α1 displayed the highest intensity in the synaptic fraction where it is known to be predominantly expressed for fast phasic GABAergic neurotransmission.

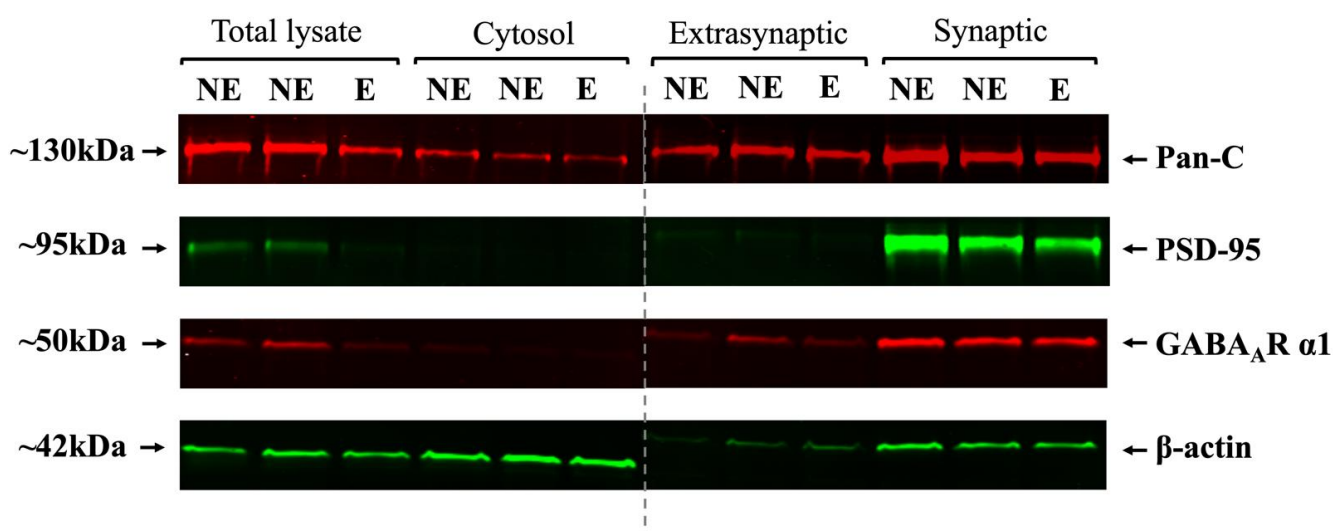


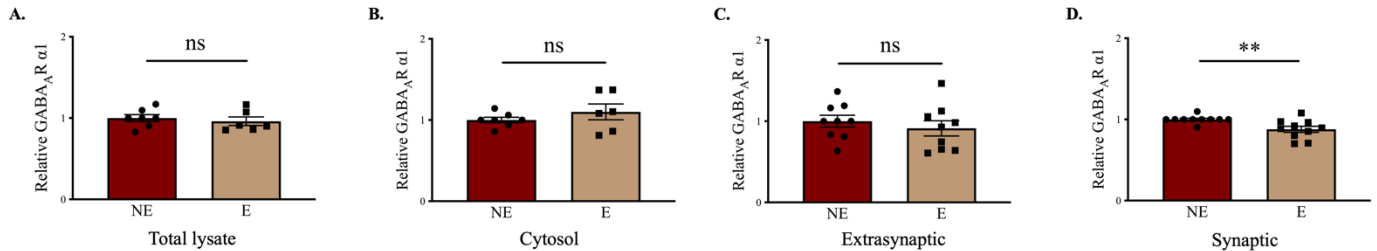
**Figure 6.** Pilot WB run for biochemically isolated primary SoCx subcellular fractions (total lysate, cytosol, extra-synaptic and synaptic). This run confirmed the successful isolation of the synaptic fractions given the intense labelling for both PSD95 and GABA<sub>A</sub>R α1. Extra-synaptic fraction, on the other hand, showed no bands for PSD95, but low intensity bands were seen for GABA<sub>A</sub>R α1 and β-actin. PanC showed good expression in all subcellular fractions.

### 2.4. Synaptic GABA<sub>A</sub>R α1 Is Significantly Reduced in Stargazer Primary SoCx with No Significant Subcellular Change in Other GABA<sub>A</sub>R Subunits

Since the stargazer primary SoCx showed a tissue reduction of GABA<sub>A</sub>R α1, it was necessary to determine whether such loss occurred in the synapses of the stargazer primary SoCx. For this purpose, biochemical fractionation technique was used to obtain subcellular fractions from primary SoCx homogenates followed by probing for GABA<sub>A</sub>R α1 using WB analysis. WB analysis of the synaptic fraction revealed a statistically significant reduction of 12.2 percent in GABA<sub>A</sub>R α1 subunit expression in stargazers compared to their NE littermates (NE:  $1.000 \pm 0.146$  [ $n = 10$ ], E:  $0.878 \pm 0.037$  [ $n = 10$ ];  $p = 0.002$ ; Figure 7D). No difference was detected in GABA<sub>A</sub>R in the other three subcellular fractions (Figure 7A–C). Biochemically isolated subcellular fractions were also probed for GABA<sub>A</sub>R α3, α4, α5, and δ. This was to reveal any altered levels that may have been masked upon WB analysis of global tissue expression. There was no significant change in the α3 subunit in any subcellular fraction from stargazer primary SoCx compared to their control littermates (Figure 7E–H). Our results also revealed no significant change in either α4 (Figure 8A–D),

$\alpha 5$  (Figure 8E–H), or  $\delta$  (Figure 8I–L) subunit levels in all the sub-cellular fractions (total lysate, cytosol, synaptic, and extra-synaptic).

(A–D) WB analyses comparing GABA<sub>A</sub>R  $\alpha 1$  levels in subcellular components from primary SoCx of the epileptic (E) stargazers and control NE littermates



(E–H) WB analyses comparing GABA<sub>A</sub>R  $\alpha 3$  levels in subcellular components from primary SoCx of the epileptic (E) stargazers and control NE littermates

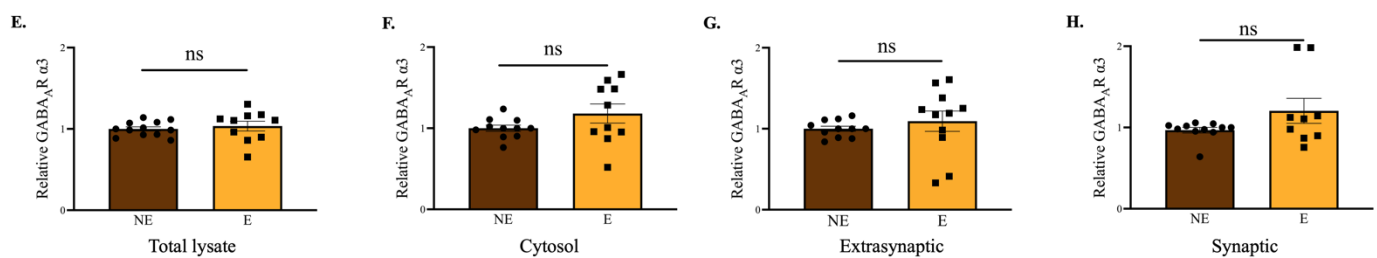


**Figure 7.** WB analyses of biochemically isolated fractions from the primary SoCx for GABA<sub>A</sub>R  $\alpha 1$  and  $\alpha 3$  subunits. Isolated subcellular fractions were compared between control (NE) littermates and epileptic (E) stargazers. (A–D) Biochemical fractionation analysis revealed a 12.2% reduction in the synaptic expression of phasic GABA<sub>A</sub>R  $\alpha 1$  in the primary SoCx of the stargazers compared to their control littermates (NE:  $1.000 \pm 0.146$  [ $n = 10$ ], E:  $0.878 \pm 0.037$  [ $n = 10$ ];  $p = 0.002$ ); no significant difference was revealed from the other subcellular components: total lysate (NE:  $1.000 \pm 0.043$  [ $n = 7$ ], E:  $0.961 \pm 0.052$  [ $n = 6$ ];  $p = 0.531$ ), cytosol (NE:  $1.000 \pm 0.034$  [ $n = 7$ ], E:  $1.100 \pm 0.098$  [ $n = 6$ ];  $p = 0.443$ ), and extra-synaptic (NE:  $1.000 \pm 0.074$  [ $n = 9$ ], E:  $0.912 \pm 0.094$  [ $n = 9$ ];  $p = 0.385$ ). (E–H) Biochemical fractionation analysis revealed no significant change in GABA<sub>A</sub>R  $\alpha 3$  in all subcellular components from the primary SoCx of stargazers compared to their control littermates: Total lysate (NE:  $1.000 \pm 0.026$  [ $n = 12$ ], E:  $1.035 \pm 0.060$  [ $n = 10$ ];  $p = 0.381$ ), cytosol (NE:  $1.000 \pm 0.037$  [ $n = 11$ ], E:  $1.181 \pm 0.118$  [ $n = 10$ ];  $p = 0.349$ ), extra-synaptic (NE:  $1.000 \pm 0.031$  [ $n = 11$ ], E:  $1.093 \pm 0.125$  [ $n = 11$ ];  $p = 0.133$ ), and synaptic (NE:  $0.967 \pm 0.034$  [ $n = 11$ ], E:  $1.205 \pm 0.153$  [ $n = 9$ ],  $p = 0.359$ ). The significance threshold was set at 0.05 with \*\* indicating  $p < 0.01$ . ‘ns’ indicates no significant change found from analyses.

(A–D) WB analyses comparing GABA<sub>A</sub>R  $\alpha 4$  levels in subcellular components from primary SoCx of the epileptic (E) stargazers and control NE littermates

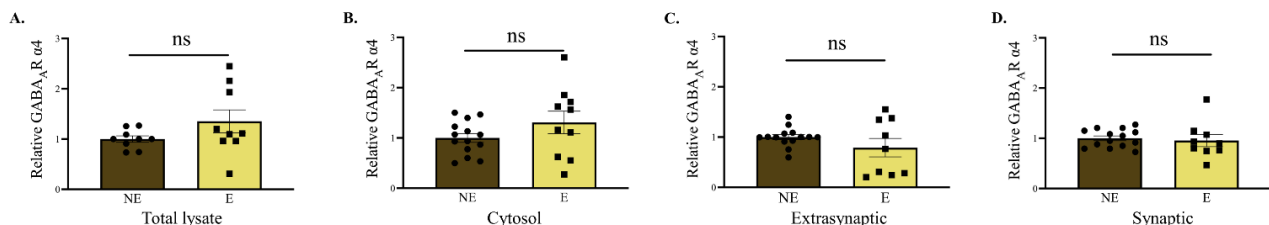


**Figure 8.** Cont.

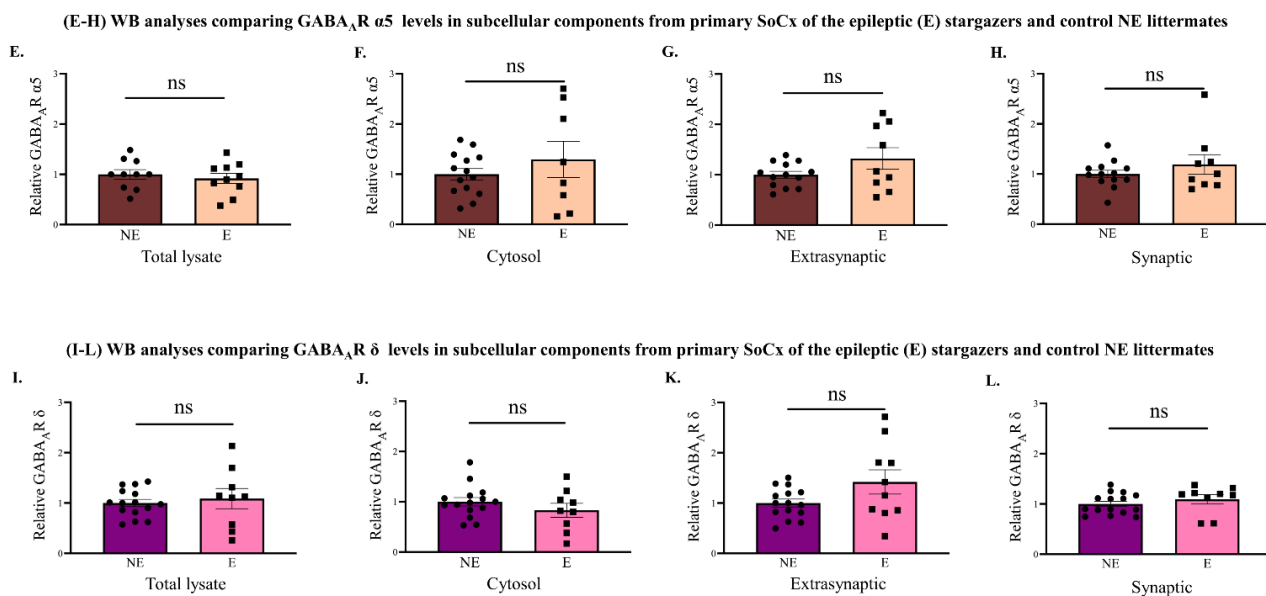


**Figure 8.** WB analyses of biochemically isolated fractions from primary SoCx for GABA<sub>A</sub>R α4, α5, and δ subunits. Subcellular fractions were isolated from the control (NE) littermates and epileptic epileptic (E) stargazers. (A–D) Biochemical fractionation analysis revealed no significant change in GABA<sub>A</sub>R α4 in all subcellular components from the primary SoCx of stargazers compared to their NE littermates: total lysate (NE:  $1.000 \pm 0.063$  [ $n = 9$ ], E:  $1.353 \pm 0.227$  [ $n = 9$ ];  $p = 0.257$ ), cytosol (NE:  $1.000 \pm 0.088$  [ $n = 14$ ], E:  $1.308 \pm 0.223$  [ $n = 10$ ];  $p = 0.172$ ), extra-synaptic (NE:  $1.000 \pm 0.051$  [ $n = 14$ ], E:  $0.789 \pm 0.183$  [ $n = 9$ ];  $p = 0.516$ ), and synaptic (NE:  $1.000 \pm 0.047$  [ $n = 14$ ], E:  $0.955 \pm 0.122$  [ $n = 9$ ];  $p = 0.369$ ). (E–H) GABA<sub>A</sub>R α5 analysis revealed no significant change in all subcellular components from the primary SoCx of stargazers compared to their control littermates: total lysate (NE:  $1.000 \pm 0.094$  [ $n = 10$ ], E:  $0.919 \pm 0.102$  [ $n = 10$ ];  $p = 0.566$ ), cytosol (NE:  $1.000 \pm 0.113$  [ $n = 14$ ], E:  $1.295 \pm 0.362$  [ $n = 8$ ];  $p = 0.920$ ), extra-synaptic (NE:  $1.000 \pm 0.068$  [ $n = 13$ ], E:  $1.324 \pm 0.214$  [ $n = 9$ ];  $p = 0.431$ ) and, synaptic (NE:  $1.000 \pm 0.075$  [ $n = 13$ ], E:  $1.190 \pm 0.195$  [ $n = 9$ ];  $p = 0.744$ ). (I–L) No statistically significant change was also seen for GABA<sub>A</sub>R δ subunit in all subcellular components from the primary SoCx of stargazers compared to their control littermates: total lysate (NE:  $1.000 \pm 0.071$  [ $n = 15$ ], E:  $1.088 \pm 0.201$  [ $n = 9$ ];  $p = 0.815$ ), cytosol (NE:  $1.000 \pm 0.083$  [ $n = 15$ ], E:  $0.831 \pm 0.138$  [ $n = 9$ ];  $p = 0.379$ ), extra-synaptic (NE:  $1.000 \pm 0.078$  [ $n = 15$ ], E:  $1.419 \pm 0.241$  [ $n = 10$ ];  $p = 0.191$ ), and synaptic (NE:  $1.000 \pm 0.053$  [ $n = 15$ ], E:  $1.092 \pm 0.094$  [ $n = 9$ ];  $p = 0.263$ ). The significance threshold was set at 0.05. ‘ns’ indicates no significant change found from analyses.

### 2.5. PV<sup>+</sup> Feed-Forward Inhibitory Interneurons Show No Overall Change in Synaptic GABA<sub>A</sub>R α1

Since biochemical fractionation revealed that GABA<sub>A</sub>R α1 was significantly reduced in synaptic fractions from stargazers, the next step was to determine if the subunit was reduced specifically at synapses between PV<sup>+</sup> feed-forward interneurons and their targets. PV<sup>+</sup> neurons synapse onto the soma, proximal dendrites, and axonal initial regions of the pyramidal cells [65], which are their primary targets in the SoCx. However, they also show a high degree of reciprocal connectivity with each other and other inhibitory interneurons [66]. Double-labelled ICC-EM of primary SoCx sections with 10 nm immunogold for GABA<sub>A</sub>R α1 and 20 nm gold for PV were used to detect GABA<sub>A</sub>R α1 at inhibitory synapses between PV<sup>+</sup> interneurons and their targets. The majority of the inhibitory synapses imaged did not have 20 nm gold particle labelling in both pre- and post-synaptic profiles. At the inhibitory synapses between these non-PV labelled neurons in the stargazer primary SoCx, there was no significant difference in the density of 10 nm gold particles label for GABA<sub>A</sub>R α1 (Figure 9A; NE:  $10.65 \pm 0.918$  [ $n = 7$ ], E:  $10.72 \pm 0.751$  [ $n = 7$ ];  $p = 0.804$ ). Gold particles/μm

at inhibitory synapses, between PV<sup>+</sup> feed-forward inhibitory terminals and their primary targets, were assessed by identifying GABA<sub>A</sub>R α1 10 nm gold-labelled synapses where PV 20 nm immunogold was restricted to presynaptic terminals. Inhibitory presynaptic terminals were identified by the presence of pleiomorphic vesicles observed as a denser and darker stained profile [67]. The combined data from all seven pairs revealed no significant difference in GABA<sub>A</sub>R α1 levels at output synapses from PV<sup>+</sup> feed-forward inhibitory neurons onto their non-PV targets (Figure 9B; NE: 11.82 ± 1.325, E: 11.15 ± 1.007,  $p > 0.999$ ).

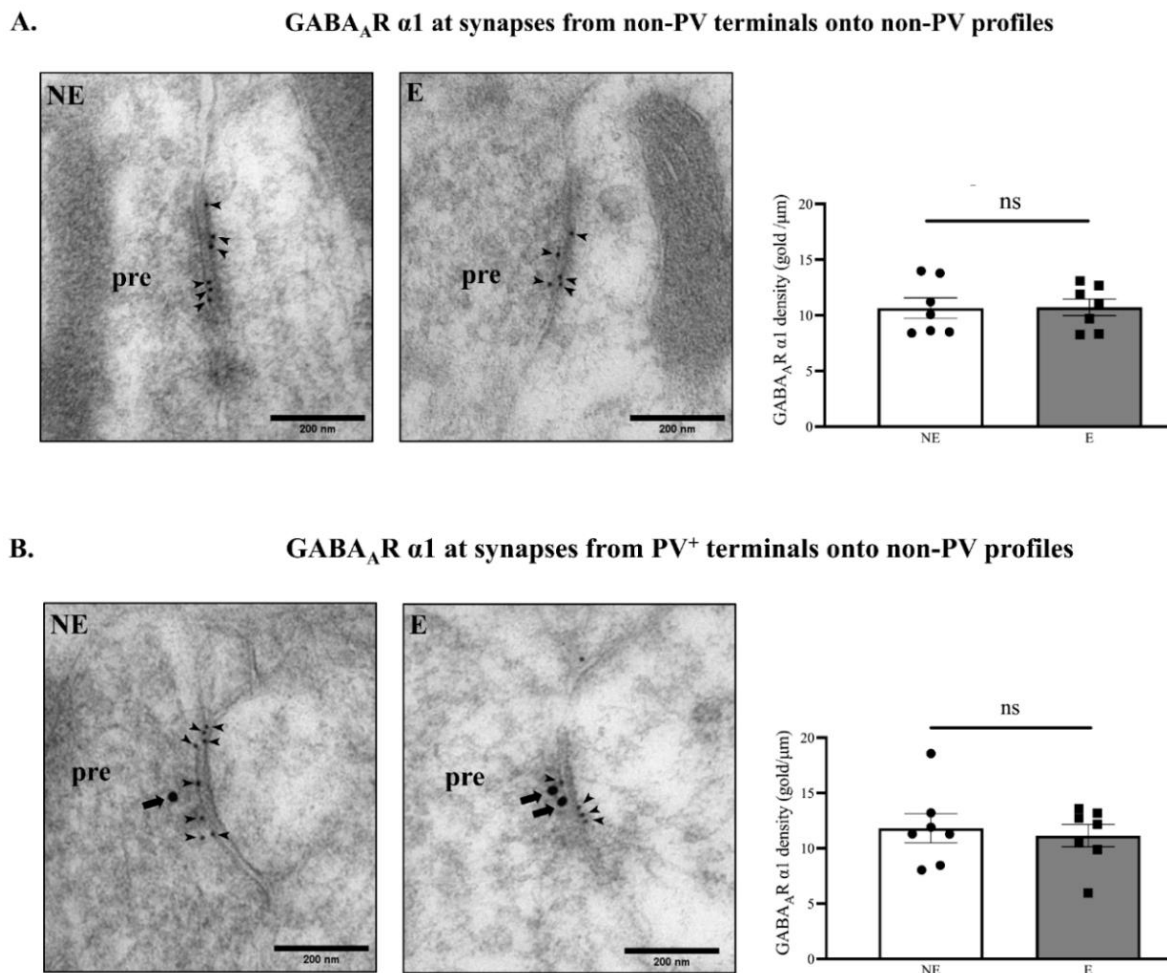


**Figure 9.** ICC-EM analysis for GABA<sub>A</sub>R α1 at PV<sup>+</sup> and non-PV inhibitory synapses in the primary SoCx compared and analyzed between control (NE) littermates and epileptic (E) stargazers. From top to bottom: Representative EM micrographs demonstrate PV labelling in the presynaptic terminals (pre), which appear darker stained, in stargazer and NE littermate primary SoCx. Arrow represents 20 nm immunogold particle labelling PV while arrowhead represents 10 nm immunogold labelling GABA<sub>A</sub>R α1. (A) For analysis for GABA<sub>A</sub>R α1 at inhibitory synapses from non-PV terminals onto non-PV profiles, as indicated by lack of 20 nm gold particles, 490 synapses in stargazers and 490 in control littermates primary SoCx were analyzed from seven pairs distributed equally. No significant difference was seen in the seven pairs (NE: 10.65 ± 0.918 [ $n = 7$ ], E: 10.72 ± 0.751 [ $n = 7$ ];  $p = 0.804$ ). (B) Analysis for GABA<sub>A</sub>R α1 at inhibitory synapses with PV (20 nm gold) in the presynaptic terminals revealed no significant difference between the stargazers (63 synapses analyzed) and control littermates (63 synapses analyzed) (NE: 11.82 ± 1.325 [ $n = 7$ ], E: 11.15 ± 1.007 [ $n = 7$ ],  $p > 0.999$ ). The significance threshold was set at 0.05. ‘ns’ indicates no significant change found from analyses.

### 3. Discussion

In this study, findings revealed for the first time a significant reduction in synaptic GABA<sub>A</sub>R α1 in the primary SoCx of the stargazer mouse model of absence epilepsy. Since

synaptic GABA<sub>A</sub>R  $\alpha$ 1 subunit is crucial for rapid inhibitory post-synaptic potentials [31,42,43], this suggests a potential reduction in overall phasic inhibition in the stargazer primary SoCx. Such a reduction would suggest an increase in the overall cortical hyperexcitability, which may contribute to the generation or maintenance of seizures. Our results also suggest a potential restructuring in the cortical GABAergic organization as our EM results revealed no significant change in GABA<sub>A</sub>R  $\alpha$ 1 levels at synapses between PV<sup>+</sup> interneurons and their targets. No concurrent changes were found in other GABA<sub>A</sub>R subunits investigated in this study, which included  $\alpha$ 3,  $\alpha$ 4,  $\alpha$ 5,  $\beta$ 2,  $\beta$ 3,  $\gamma$ 2, and  $\delta$ . It is possible that efficient reorganization of the subunits in GABA<sub>A</sub>R pentamer masks any changes and thus were not detectable with the techniques utilized in this study.

### 3.1. Altered Synaptic GABA<sub>A</sub>R $\alpha$ 1 Expression in the Stargazer Primary SoCx

In the current study, we report a statistically significant but small reduction only in the synaptic expression of GABA<sub>A</sub>R  $\alpha$ 1 subunit in the primary SoCx of the stargazer mouse model. We found no concurrent changes in  $\alpha$ 1 expression at either extra-synaptic site where it is also found [68], or intracellularly, where synthesis and protein assembly occur. This differs from findings in the heterozygous GABA<sub>A</sub>R  $\alpha$ 1 knock-out mouse model of absence epilepsy where a concurrent reduction in tissue and surface expression of the subunit has been reported [12]. Furthermore, in the GABA<sub>A</sub>R  $\alpha$ 1 knock-out mouse model of absence epilepsy [12,46], a loss of the  $\alpha$ 1-subunit is associated with altered expression of other GABA<sub>A</sub>R subunits co-expressed with  $\alpha$ 1, suggesting a rearrangement of the pentameric structure inevitably resulting in altered inhibitory dynamics. In such mice, concurrent increases in cortical levels of  $\alpha$ 2 and  $\alpha$ 3, reductions in cortical levels of GABA<sub>A</sub>R  $\beta$ 2,  $\beta$ 3, and  $\gamma$ 2, and cortical layer-specific reduction in peak inhibitory postsynaptic currents have been reported [12,46]. Similar concurrent changes in GABA<sub>A</sub>R subunits have also been reported in the Wistar Albino Glaxo from Rijswijk rat (WAG/Rij) which shows significant reduction in cortical GABA<sub>A</sub>R  $\alpha$ 1,  $\beta$ 3, and  $\gamma$ 2 [69], perhaps correlated to the significant reduction in cortical inhibition reported in these rats [70,71]. In the stargazer primary SoCx, however, similar changes were not seen in the GABA<sub>A</sub>R subunits ( $\alpha$ 3,  $\beta$ 2,  $\beta$ 3, and  $\gamma$ 2) investigated that show co-expression with synaptic GABA<sub>A</sub>R  $\alpha$ 1. A reason for this could be that the marginal reduction in  $\alpha$ 1 induces only modest compensatory changes in the other synaptic GABA<sub>A</sub>R subunits, such that these changes are not detectable as significantly altered expressions.

Synaptic  $\alpha$ 1-containing GABA<sub>A</sub>Rs are the principal mediators of fast synaptic inhibition [31,42,43], comprising nearly 40–60% of cortical GABA<sub>A</sub>Rs with preferential perisomatic and peripheral dendritic expression at PV<sup>+</sup> inputs onto principal pyramidal neurons and other PV<sup>+</sup> interneurons [42,72]. GABA<sub>A</sub>R  $\alpha$ 1 subunit loss on principal pyramidal neurons would potentially increase their excitability. Conversely, such a loss on PV<sup>+</sup> somas and dendrites themselves would potentially cause increased inhibition of target pyramidal neurons due to the disinhibitory effect in PV<sup>+</sup> interneurons. Reports suggest that downregulation of  $\alpha$ 1-containing GABA<sub>A</sub>Rs and GABAergic inputs, in response to reduced excitatory input on inhibitory interneurons, preferentially occurs in pyramidal neurons [73,74]. In the stargazer, a loss in GABA<sub>A</sub>R  $\alpha$ 1 in pyramidal neurons could be attributed to a downstream effect of dysfunctional PV<sup>+</sup> inhibitory interneurons or even increased internalization of GABA<sub>A</sub>Rs in response to enhanced neuronal excitability [75].

### 3.2. GABA<sub>A</sub>R $\alpha$ 1 Is Not Altered at Synapses from PV<sup>+</sup> Interneurons Onto Targets

Although the current study discovered a loss of synaptic GABA<sub>A</sub>R  $\alpha$ 1 in the stargazer primary SoCx when analyzed in the whole tissue protein homogenate, results from EM revealed no change in  $\alpha$ 1 density within each inhibitory synapse from PV<sup>+</sup> terminals onto non-PV targets. It is highly possible that altered  $\alpha$ 1 subunit density within inhibitory synapses is cortical layer-specific, which was not investigated in this study. Cortical layer-specific changes in inhibition have been reported in other rodent models of absence seizures [11,76,77]. A second possibility is a change in the morphology of GABAergic

neurons as a result of loss of excitatory input, which potentially alters the number of synapses but not the density of  $\alpha 1$  subunit within each synapse. Such a reduction has been reported in the stargazer cerebellum as well [78]. Indeed, altered strength of excitatory inputs can bring adaptive changes in inhibitory GABAergic networks [79], which could potentially augment the loss of appropriate inhibitory inputs onto target neurons, leading to other downstream changes because of increased excitability. Developmentally, in mice, fast-spiking activity of PV<sup>+</sup> interneurons engage by day 18, which interestingly in stargazers coincides with the onset of SWDs [17]. It is likely that in the stargazers, dysfunctional PV<sup>+</sup>-mediated FFI triggers mechanisms that translate into reduced overall GABA<sub>A</sub>R  $\alpha 1$  expression. It should be emphasized that although synaptic GABA<sub>A</sub>R  $\alpha 1$  is largely expressed around PV<sup>+</sup> interneurons and is likely reduced around these interneurons, given the stargazer's dysfunctional PV<sup>+</sup>-mediated FFI, the possibility of differential effects between other populations of cortical neurons cannot be excluded.

### 3.3. Impact of Altered Cortical Inhibition

Recently members of our lab demonstrated that independently silencing PV<sup>+</sup> interneurons in both the cortex and RTN using DREADD technology in freely moving mice produced absence-like SWDs [23,80]. This recaptures the dysfunctional FFI of the stargazer mouse where PV<sup>+</sup> interneurons of the CTC network are affected by loss of AMPA receptors [20–22]. However, unlike acutely induced change in the DREADD mice, the stargazers present with a chronic loss of excitation (via loss of AMPA receptors activity) at PV<sup>+</sup> interneurons concurrently in the primary SoCx and the RTN. In the RTN, increased activity of NMDA receptors has been reported in stargazers [81], albeit in the absence of altered NMDA receptors expression [63], perhaps as a compensatory glutamatergic activation of NMDA receptors in the absence of AMPA receptors [82]. Likewise, the increase in GABA<sub>A</sub>R subunits expression in the thalamic relay neurons post-seizure onset [28–30] may also be a compensatory consequence of reduced RTN-mediated inhibition, which preferentially targets VP thalamic nucleus [83]. In this context, recently it was reported that in the freely moving Genetic Absence Epilepsy Rat from Strasbourg (GAERS), the large majority of thalamocortical relay neurons remain silent during SWDs with few displaying increased phasic and tonic inhibition as a result of burst activity from the RTN, which is activated by top-down cortical excitations [37]. Indeed, recent computational modelling studies further demonstrate the suppressive role of intra-thalamic phasic and tonic inhibition during SWDs [84].

As for the SoCx, reports from different animal models suggest both enhanced inhibition as well as reduced inhibitory activity [16,32]. Layer-specific reduced inhibition has been reported in various animal models including: the WAG/Rij, which displays reduced expression of PV<sup>+</sup> interneurons in the primary SoCx [76]; a mouse model of a human genetic absence epilepsy syndrome [12], which shows reduced inhibitory postsynaptic currents in layer VI of sensory cortex; and the knock-in  $\gamma 2R43Q$  mouse model with a point mutation in GABA<sub>A</sub>R  $\gamma 2$ , which presents with reduced inhibitory currents in pyramidal neurons [11]. In the GAERS, however, reports suggest an increase in cortical inhibition as a result of increased cortical GABA<sub>B</sub> receptor expression, which contributes to tonic inhibition [34,85]. GAERS also have layer-specific increases in PV<sup>+</sup> (layer V) and SOM<sup>+</sup> (Layer IV) inhibitory interneurons [76,77], and increased expression of stargazin and AMPA receptors [86,87]. It should be noted that increased inhibition in the cortex could paradoxically lead to increased excitability via activation of disinhibitory circuits [88,89]. Reports in GAERS do indicate increased neuronal excitabilities in deep cortical layers associated with absence seizures [38,90]. Given the complexity of the cortical inhibitory microcircuits, a loss of cortical PV<sup>+</sup>-mediated FFI coupled with a further loss of phasic inhibition could cause increased excitability of principal excitatory neurons, which then leads to hyper-activation of disinhibitory motifs with subsequent downstream saturation of the extracellular space with GABA neurotransmitter. Any increase in extracellular ambient GABA would translate into increased tonic inhibition by activation of extra-synaptic GABA<sub>A</sub>Rs. Interestingly, we

recently reported a significant increase in total GABA levels in the stargazer SoCx using HPLC, but a decrease in GABA expression within presynaptic terminals [91]. Moreover, we also found a significant increase in the GAD65 enzyme, but not GAD67 or GAT-1 (GABA Transporter-1) in the same region [92]. GAD65 is chiefly localized in the axon terminals [93], with increased GABA synthesis during intense synaptic activity mediated by this enzyme [94]. These findings substantiate the inference that there may be an extracellular increase in GABA in the epileptic primary SoCx.

### 3.4. Conclusions

Mounting evidence suggests the importance of GABAergic inhibitory malfunction in the pathogenesis of absence seizures [1]. In this study, we primarily aimed to investigate changes in the ubiquitous GABA<sub>A</sub>R  $\alpha$ 1 subunit as a means of investigating GABA<sub>A</sub>R expression in the primary SoCx of the stargazer mouse model of absence epilepsy. GABA<sub>A</sub>R-mediated phasic and tonic inhibitory currents are integral to the physiological E/I balance of neuronal circuits and any change can alter the function, kinetics, and pharmacology of GABA<sub>A</sub>Rs [79]. GABA<sub>A</sub>R plasticity is a natural response of neuronal circuits perhaps as an attempt to balance hyperexcitability, but such changes can themselves contribute to further pathogenesis of the original disorder [95]. A loss of the GABA<sub>A</sub>R  $\alpha$ 1 subunit has been reported in the literature, both in human patients [96,97], as well as in genetic absence seizure animal models used in research. In the stargazer, loss of FFI coupled with the loss of synaptic GABA<sub>A</sub>R  $\alpha$ 1 could lead to enhanced excitability of target principal pyramidal neurons. EM assessment in this study, which analyzed GABA<sub>A</sub>R  $\alpha$ 1 subunit density within synapses (immunogold/ $\mu$ m length of synapse), revealed no change in the  $\alpha$ 1 subunit expression within the inhibitory synapses investigated. Conversely, semi-quantitative WB analyses, which analyzed the subunit collectively at all synapses in the primary SoCx, revealed reduced  $\alpha$ 1 subunit expression. This could reflect a change in the number of inhibitory synapses or altered GABAergic connectivity from cortical GABAergic interneurons. The resulting enhanced cortical excitability could potentially alter the glutamate and GABA neurotransmitter dynamics that may exacerbate seizure generation. In the stargazer mouse model, genetic mutation has not only been associated with altered expression of GABA<sub>A</sub>Rs, but altered GABA neurotransmitter dynamics as well [34,78], which in turn can affect the development of neurons, synapses, and the expression of GABA<sub>A</sub>Rs themselves [98]. Further in-depth investigations into discerning the specific changes in GABAergic neurotransmission could be crucial for enabling development of targeted preventative and treatment strategies.

## 4. Materials and Methods

### 4.1. Animals

The Stargazer mice (*B6C3Fe a/a-Cacng<sup>2stg</sup>/J*) used in this study were derived from breeding stocks obtained from the Jackson Laboratory (Bar Harbor, ME, USA). Adult 8–12-week-old epileptic (E) stargazers (*stg/stg*) and their NE (heterozygous [*Het*, *+/stg*] and wild-type [*WT*, *+/+*]) control littermates were raised at the University of Otago's Animal Resource Unit. The mice had ad libitum access to food and were housed in well-ventilated cages with optimum environmental conditions (12 h light/dark cycle, temperature  $\sim$ 21 °C and  $\sim$ 50% humidity). Genotypes were confirmed from ear-notches taken post-sacrifice using common forward (TAC TTC ATC CGC CAT CCT TC), wild-type reverse (TGG CTT TCA CTG TCT GTT GC), and mutant reverse (GAG CAA GCA GGT TTC AGG C) primer sequences. All animal procedures were carried out according to the University of Otago Animal Ethics Committee approved protocols and guidelines (32/16). A total of 142 animals (77 NE control littermates and 65 epileptic stargazers) were used for all the experiments in this study. The 'n' numbers represent the sample numbers used within each experiment.

#### 4.2. Immunofluorescence Confocal Microscopy

Animals (3 control littermates and 3 stargazer mice) were perfuse-fixed with 4% PFA and brains extracted for confocal microscopy as previously described [28]. Following overnight post-fixation at 4 °C and cryoprotection in increasing concentrations of sucrose, the brains were coronally sectioned at 30 µm in a freezing cryostat. Brain slices were selected from the primary SoCx regions based on bregma points [99], from anterior (1.10 to 0.02), mid (0.02 to −0.82), and posterior (−0.82 to −1.70) regions. The sections were triple-labelled with GABA<sub>A</sub>R α1 (1:500; AGA-001, Alomone, Jerusalem, Israel), PV (1:2000; PV 235, Swant, Burgdorf, Switzerland), and VGlut2 (1:500; 135404, Synaptic Systems, Goettingen, Germany). Sections were labelled for GABA<sub>A</sub>R α1 to confirm its distribution in the stargazer primary SoCx against NE littermates and to confirm the presence of α1 subunit across the layers. The tissue was also probed for PV protein to assist in recognizing GABA<sub>A</sub>R α1 in PV<sup>+</sup> neurons [21]. To help distinguish the cortical layers, the tissue was also labelled for VGlut2, which causes intense labelling of thalamocortical projections in layer IV [49,51,100], and has previously been used by us for the same purpose [21]. GABA<sub>A</sub>R α1 pre-adsorption and omission control sections were processed in parallel (Supplementary Figure S1). After development of immunofluorescence with Alexa Fluor 568 (1:1000; A-11031, Life Technologies, CA, USA), Alexa Fluor 488 (1:1000; A-11008, Life Technologies, CA, USA), and Alexa Fluor 633 (1:1000, A21105, Life Technologies, CA, USA), images were acquired using Nikon A1+ Inverted Confocal Laser Scanning Microscope. The following channel configuration was used: green channel 488 nm for GABA<sub>A</sub>R α1, red channel 543 nm laser for PV and blue channel 633 nm laser for VGlut2. Z-stacks of primary SoCx were taken from each section at different planes, with the aim of at acquiring between 6 and 9 images in each stack. Optimal planes were determined by the brightest fluorescence. Laser intensity, gain, and offset were determined using the white matter and maintained across all image acquisition. The numerical aperture was kept at 1.3, pinhole size was set to 1 AU, and z-axis step-size was chosen as 1 µm. Image format was acquired at 1024 × 1024 pixels for 10× magnification (Objective: 10× Plan), and 512 × 512 for 60× magnification (Objective: 60× PlanApo oil). Images were observed using ImageJ software (NIH, Bethesda, MD, USA). Channels were first split and then enhanced using ImageJ Z-project and flatten functions.

#### 4.3. Western Blotting

Mice were decapitated after sacrifice through cervical dislocation, brains extracted and snap-frozen on dry ice. Brains were sectioned in a cryostat (Leica CM1950, Leica Microsystems, Wetzlar, Germany), maintained at −10 °C, and 300 µm thick coronal sections produced, which were thaw-mounted onto glass slides followed by microdissection of the primary SoCx region out of each section between bregma 1.09 to bregma −1.91. Tissue samples obtained were subsequently processed for Western blotting. Briefly, micro-dissected tissue samples were immediately placed into lysis buffer (0.5 M Tris-base, 100 mM EDTA, 3% SDS, pH6.8) supplemented with 1% phenylmethyl sulfonyl fluoride (PMSF) and 1% protease inhibitor (P8340, Sigma-Aldrich, St. Louis, MO, USA). Tissue samples were homogenized via sonication, heated for 2 min at 100 °C, and centrifuged at 13,000 RPM for 5 min in a chilled centrifuge (4 °C) to extract the supernatants, which were stored at −80 °C. The samples were quantified for protein content using detergent-compatible colorimetric assay (DC Protein Assay, 500, 0116, Bio-Rad, Hercules, CA, USA). The protein content in the samples were separated in an 8.5% resolving gel using SDS-PAGE, followed by transfer onto nitrocellulose membranes. Membranes were probed using GABA<sub>A</sub>R α1 (1:500; AGA-001, Alomone, Jerusalem, Israel), GABA<sub>A</sub>R α3 (1:500; AGA-003, Alomone, Jerusalem, Israel), GABA<sub>A</sub>R α4 (1:200; AGA-008, Alomone, Jerusalem, Israel), GABA<sub>A</sub>R α5 (1:1000; AB9678, Sigma-Aldrich, St. Louis, MO, USA), GABA<sub>A</sub>R β2 (1:1000; ab8340, Abcam, Cambridge, UK), GABA<sub>A</sub>R β3 (1:1000; ab4046, Abcam, Cambridge, UK), GABA<sub>A</sub>R γ2 (1:200; AGA-005, Alomone, Jerusalem, Israel), and GABA<sub>A</sub>R δ (1:200; AGA-014, Alomone, Jerusalem, Israel) with β-actin (1:1000; ab8226, Abcam, Cambridge UK) used

for normalization. After enhancement of immunofluorescence with IRDye800CW (1:1000; 926-32221, LI-COR Biosciences, Lincoln, NE, USA) and IRDye680 (1:1000; 926-32210, LI-COR Biosciences, Lincoln, NE, USA) secondary antibodies, membranes were scanned using Odyssey Infrared Imager (Li-Cor Biosciences, Lincoln, NE, USA) and protein bands were analyzed for integrated intensity using Odyssey v3.1 software (Li-COR Biosciences, Lincoln, NE, USA). Representative full blots are provided in supplementary Figure S2 (GABA<sub>A</sub>R  $\alpha$ 1 and  $\alpha$ 3), Figure S3 (GABA<sub>A</sub>R  $\beta$ 2,  $\beta$ 3, and  $\gamma$ 2), and Figure S4 (GABA<sub>A</sub>R  $\alpha$ 4,  $\alpha$ 5 and  $\delta$ ). GABA<sub>A</sub>R subunit intensity values were normalized against  $\beta$ -actin control bands, and ratios of the normalized intensities against mean normalized values of NE littermates within each litter was calculated before statistical testing and graphical representation of data.

#### 4.4. Biochemical Fractionation

Primary SoCx microdissections were obtained from snap-frozen brains extracted from animals using the same process as described for Western blotting. Tissue samples were homogenized in ice-cold fractionation buffer (320 mM sucrose, 10 mM tris-base, 1 mM EDTA, pH 7.37) supplemented with PMSF and protease inhibitor using sterile plastic pestles and sonication. A multistep centrifugation technique was used to isolate subcellular fractions from homogenized samples as previously described [20]. Briefly, each tissue sample was centrifuged at  $1000\times g$  for 10 min to obtain supernatant (total lysate), followed by further centrifugation of the extracted supernatant at  $10,000\times g$  for 15 min to separate out the membrane component as pellet. The fresh supernatant was separated out as cytosol fraction, while the membrane pellet was re-suspended in homogenization buffer (50 mM Tris, 2 mM EDTA, 3% SDS, pH 6.8) containing triton X-100, followed by incubation on ice for 40 min, and centrifugation at  $32,000\times g$  for 30 min to isolate the synaptic component as pellet. This separation depends on the insolubility of the synaptic densities in triton X-100. The supernatant-containing extra-synaptic component was extracted while the pellet was re-suspended in the homogenization buffer. The supernatant (extra-synaptic fraction) was mixed overnight with acetone, followed by 15 min  $3000\times g$  centrifugation to isolate the extra-synaptic component as pellet which was re-suspended in the homogenization buffer. The subcellular fractions were processed and analyzed as described above in Section 4.3. PanC (1:1000; 4068P, Cell Signaling Technology, Danver, MA, USA) was added for normalization and analyses while PSD-95 (1:1000; 124011, Synaptic Systems, Goettingen, Germany) and  $\beta$ -actin were used as additional controls. Representative full blots are provided in Supplementary Figure S5 (GABA<sub>A</sub>R  $\alpha$ 1 and  $\alpha$ 3) and Figure S6 (GABA<sub>A</sub>R  $\alpha$ 4,  $\alpha$ 5 and  $\delta$ ). The purity of the subcellular fractions was assessed (Figure 6). The GABA<sub>A</sub>R subunit intensities were normalized against Pan-C followed by relative ratios of the normalized intensities against mean normalized values of NE littermates within each litter calculated before statistically comparing stargazers against control littermates.

#### 4.5. ICC-EM

Seven pairs of control littermates and epileptic stargazers were selected for this technique. The experiment was conducted with the researcher blinded to the identity of the samples. Samples were prepared as described previously [19,20,28,91]. Briefly, animals were sacrificed by trans-cardiac perfusion with 4% PFA and 0.1% glutaraldehyde in 0.1 M phosphate buffer (PB). The extracted brains were post-fixed in 4% PFA/0.1% glutaraldehyde followed by obtaining 250  $\mu$ m thick coronal sections. Next, 1 mm wide micro-punches were taken from full thickness primary SoCx. Ultrathin sections mounted on formvar-coated nickel grids were prepared after sequential freeze-slamming, ultra-low temperature dehydration, cryo-substitution, and embedding in lowicryl HM20 resin of the tissue samples. Grid-mounted tissue was etched with sodium ethanolate for 3 s followed by blocking in 10% NGS for 2 h and overnight incubation in a primary antibodies cocktail of GABA<sub>A</sub>R  $\alpha$ 1 (1:50; AGA-001, Alomone, Jerusalem, Israel) and PV (1:50; 235, Swant, Burgdorf, Switzerland) to conduct double-labelling. The primary antibodies were

probed with 10 nm immunogold (1:20; British Biocell International, Cardiff, UK) and 20 nm immunogold (1:20; British Biocell International, Cardiff, UK) secondary antibodies for GABA<sub>A</sub>R  $\alpha$ 1 and PV, respectively. The tissue was stained with uranyl acetate and lead citrate before imaging using a transmission electron microscope (Phillips CM100, Phillips/FEI corporation, Eindhoven, Holland). Grids were imaged at lower magnification to ascertain the layout of the tissue. This was followed by sequential imaging of synapses at high magnification. Inhibitory synapses were identified by their symmetrically thin, dense membrane ultrastructure, as can be seen in Figure 8. Excitatory synapses with their asymmetrical postsynaptic densities were clearly distinguishable from their inhibitory counterparts. Unbiased sampling was conducted throughout the tissue specimens by imaging all GABA<sub>A</sub>R  $\alpha$ 1-positive inhibitory synapses with at least 40 imaged for each animal. Synapses were subsequently analyzed in conjunction with PV<sup>+</sup> profiles. Using ImageJ, the length of each inhibitory synapse was measured while counting all 10 nm gold particles confined to within 30 nm of synaptic density. Density of GABA<sub>A</sub>R  $\alpha$ 1 was obtained by dividing the number of gold particles against the length of synapses in which they were found.

#### 4.6. Statistical Analyses

Data were statistically analyzed using unpaired non-parametric Mann–Whitney U test for comparison between the two independent groups of control littermates and epileptic stargazers in the same population. Independent variability between the two groups is the existence of genetic mutation-based phenotype in the stargazers and lack thereof in the control group. Data from stargazers were first normalized against the controls before transferring into GraphPad Prism (GraphPad Software Inc., San Diego, CA, USA) for statistical analysis with statistical significance defined as:  $p < 0.05$  as \*;  $p < 0.01$  as \*\*;  $p < 0.001$  as \*\*\*. The data in this study have been presented as mean  $\pm$  standard error of mean (SEM).

**Supplementary Materials:** The supporting information can be downloaded at: <https://www.mdpi.com/article/10.3390/ijms232415685/s1>.

**Author Contributions:** B.L. conceptualized and designed the research, supervised the project, and secured the funding. N.K.A. helped with research design and supervision of experiments. M.H. conducted the experiments and wrote the first draft of the manuscript. Analyses and interpretation of data were conducted jointly. All authors contributed to the manuscript writing and approved the final version. All authors have read and agreed to the published version of the manuscript.

**Funding:** The research was supported by funding from the University of Otago to B.L.

**Institutional Review Board Statement:** The study was conducted according to guidelines approved on 20/11/2017 by the University of Otago Animal Ethics Committee under the AEC no. DET 32/17.

**Informed Consent Statement:** Not applicable.

**Data Availability Statement:** Data are accessible upon reasonable request.

**Acknowledgments:** The authors acknowledge the University of Otago research funding and publishing bursary awarded to B.L. and M.H., respectively.

**Conflicts of Interest:** The authors declare that the research was conducted in the absence of commercial or financial relationships that could be construed as a potential conflict of interest.

## References

1. Crunelli, V.; Lorincz, M.L.; McCafferty, C.; Lambert, R.C.; Leresche, N.; Di Giovanni, G.; David, F. Clinical and experimental insight into pathophysiology, comorbidity and therapy of absence seizures. *Brain* **2020**, *143*, 2341–2368. [[CrossRef](#)] [[PubMed](#)]
2. Blumenfeld, H. Cellular and network mechanisms of spike-wave seizures. *Epilepsia* **2005**, *46*, 21–33. [[CrossRef](#)] [[PubMed](#)]
3. Kessler, S.K.; McGinnis, E. A Practical Guide to Treatment of Childhood Absence Epilepsy. *Paediatr. Drugs* **2019**, *21*, 15–24. [[CrossRef](#)]

4. McCormick, D.A.; Contreras, D. On the cellular and network bases of epileptic seizures. *Annu. Rev. Physiol.* **2001**, *63*, 815–846. [[CrossRef](#)]
5. Cossette, P.; Liu, L.D.; Brisebois, K.; Dong, H.H.; Lortie, A.; Vanasse, M.; Saint-Hilaire, J.M.; Carmant, L.; Verner, A.; Lu, W.Y.; et al. Mutation of GABRA1 in an autosomal dominant form of juvenile myoclonic epilepsy. *Nat. Genet.* **2002**, *31*, 184–189. [[CrossRef](#)]
6. Maljevic, S.; Krampfl, K.; Rebstock, J.; Tilgen, N.; Weber, Y.G.; Cossette, P.; Rouleau, G.; Bufler, J.; Lerche, H.; Heils, A. A de novo mutation of the GABA(A) receptor alpha1-subunit associated with childhood absence epilepsy in a single patient. *Epilepsia* **2004**, *45*, 119.
7. Baulac, S.; An-Gourfinkel, I.; Prud'homme, J.F.; Baulac, M.; Bruzzone, R.; Brice, A.; Le Guern, E. First genetic evidence of GABA(A) receptor dysfunction in epilepsy. *M S-Med. Sci* **2001**, *17*, 908–909. [[CrossRef](#)]
8. Wallace, R.H.; Marini, C.; Petrou, S.; Harkin, L.A.; Bowser, D.N.; Panchal, R.G.; Williams, D.A.; Sutherland, G.R.; Mulley, J.C.; Scheffer, I.E.; et al. Mutant GABA(A) receptor gamma2-subunit in childhood absence epilepsy and febrile seizures. *Nat. Genet.* **2001**, *28*, 49–52. [[CrossRef](#)]
9. Harkin, L.A.; Bowser, D.N.; Dibbens, L.M.; Singh, R.; Phillips, F.; Wallace, R.H.; Richards, M.C.; Williams, D.A.; Mulley, J.C.; Berkovic, S.F.; et al. Truncation of the GABA(A)-receptor gamma 2 subunit in a family with generalized epilepsy with febrile seizures plus. *Am. J. Hum. Genet.* **2002**, *70*, 530–536. [[CrossRef](#)]
10. Kananura, C.; Haug, K.; Sander, T.; Runge, U.; Gu, W.L.; Hallmann, K.; Rebstock, J.; Heils, A.; Steinlein, O.K. A splice-site mutation in GABRG2 associated with childhood absence epilepsy and febrile convulsions. *Arch. Neurol.* **2002**, *59*, 1137–1141. [[CrossRef](#)]
11. Tan, H.O.; Reid, C.A.; Single, F.N.; Davies, P.J.; Chiu, C.; Murphy, S.; Clarke, A.L.; Dibbens, L.; Krestel, H.; Mulley, J.C.; et al. Reduced cortical inhibition in a mouse model of familial childhood absence epilepsy. *Proc. Nat. Acad. Sci. USA* **2007**, *104*, 17536–17541. [[CrossRef](#)] [[PubMed](#)]
12. Zhou, C.; Huang, Z.; Ding, L.; Deel, M.E.; Arain, F.M.; Murray, C.R.; Patel, R.S.; Flanagan, C.D.; Gallagher, M.J. Altered cortical GABAA receptor composition, physiology, and endocytosis in a mouse model of a human genetic absence epilepsy syndrome. *J. Biol. Chem.* **2013**, *288*, 21458–21472. [[CrossRef](#)] [[PubMed](#)]
13. Zhou, C.; Ding, L.; Deel, M.E.; Ferrick, E.A.; Emeson, R.B.; Gallagher, M.J. Altered intrathalamic GABA(A) neurotransmission in a mouse model of a human genetic absence epilepsy syndrome. *Neurobiol. Dis.* **2015**, *73*, 407–417. [[CrossRef](#)] [[PubMed](#)]
14. Witsch, J.; Golkowski, D.; Hahn, T.T.; Petrou, S.; Spors, H. Cortical alterations in a model for absence epilepsy and febrile seizures: In vivo findings in mice carrying a human GABA(A)R gamma2 subunit mutation. *Neurobiol. Dis.* **2015**, *77*, 62–70. [[CrossRef](#)] [[PubMed](#)]
15. Currie, S.P.; Luz, L.L.; Booker, S.A.; Wyllie, D.J.; Kind, P.C.; Daw, M.I. Reduced local input to fast-spiking interneurons in the somatosensory cortex in the GABAA gamma2 R43Q mouse model of absence epilepsy. *Epilepsia* **2017**, *58*, 597–607. [[CrossRef](#)]
16. Crunelli, V.; Cope, D.W.; Terry, J.R. Transition to absence seizures and the role of GABA(A) receptors. *Epilepsy Res.* **2011**, *97*, 283–289. [[CrossRef](#)]
17. Letts, V.A. Stargazer—A mouse to seize! *Epilepsy Curr.* **2005**, *5*, 161–165. [[CrossRef](#)]
18. Letts, V.A.; Felix, R.; Biddlecome, G.H.; Arikath, J.; Mahaffey, C.L.; Valenzuela, A.; Bartlett, F.S., 2nd; Mori, Y.; Campbell, K.P.; Frankel, W.N. The mouse stargazer gene encodes a neuronal Ca2+-channel gamma subunit. *Nat. Genet.* **1998**, *19*, 340–347. [[CrossRef](#)]
19. Barad, Z.; Shevtsova, O.; Arbuthnott, G.W.; Leitch, B. Selective loss of AMPA receptors at corticothalamic synapses in the epileptic stargazer mouse. *Neuroscience* **2012**, *217*, 19–31. [[CrossRef](#)]
20. Adotevi, N.K.; Leitch, B. Synaptic Changes in AMPA Receptor Subunit Expression in Cortical Parvalbumin Interneurons in the Stargazer Model of Absence Epilepsy. *Front. Mol. Neurosci.* **2017**, *10*, 434. [[CrossRef](#)]
21. Adotevi, N.K.; Leitch, B. Alterations in AMPA receptor subunit expression in cortical inhibitory interneurons in the epileptic stargazer mutant mouse. *Neuroscience* **2016**, *339*, 124–138. [[CrossRef](#)] [[PubMed](#)]
22. Adotevi, N.K.; Leitch, B. Cortical expression of AMPA receptors during postnatal development in a genetic model of absence epilepsy. *Int. J. Dev. Neurosci.* **2018**, *73*, 19–25. [[CrossRef](#)] [[PubMed](#)]
23. Panthi, S.; Leitch, B. The impact of silencing feed-forward parvalbumin-expressing inhibitory interneurons in the cortico-thalamocortical network on seizure generation and behaviour. *Neurobiol. Dis.* **2019**, *132*, 104610. [[CrossRef](#)]
24. Panthi, S.; Leitch, B. Chemogenetic Activation of Feed-Forward Inhibitory Parvalbumin-Expressing Interneurons in the Cortico-Thalamocortical Network During Absence Seizures. *Front. Cell. Neurosci.* **2021**, *15*, 688905. [[CrossRef](#)] [[PubMed](#)]
25. Payne, H.L.; Connelly, W.M.; Ives, J.H.; Lehner, R.; Furtmuller, B.; Sieghart, W.; Tiwari, P.; Lucocq, J.M.; Lees, G.; Thompson, C.L. GABAA alpha6-containing receptors are selectively compromised in cerebellar granule cells of the ataxic mouse, stargazer. *J. Biol. Chem.* **2007**, *282*, 29130–29143. [[CrossRef](#)]
26. Qiao, X.; Hefti, F.; Knusel, B.; Noebels, J.L. Selective failure of brain-derived neurotrophic factor mRNA expression in the cerebellum of stargazer, a mutant mouse with ataxia. *J. Neurosci.* **1996**, *16*, 640–648. [[CrossRef](#)] [[PubMed](#)]
27. Thompson, C.L.; Tehrani, M.H.; Barnes, E.M., Jr.; Stephenson, F.A. Decreased expression of GABAA receptor alpha6 and beta3 subunits in stargazer mutant mice: A possible role for brain-derived neurotrophic factor in the regulation of cerebellar GABAA receptor expression? *Brain Res. Mol. Brain Res.* **1998**, *60*, 282–290. [[CrossRef](#)]
28. Seo, S.; Leitch, B. Altered thalamic GABAA-receptor subunit expression in the stargazer mouse model of absence epilepsy. *Epilepsia* **2014**, *55*, 224–232. [[CrossRef](#)]

29. Seo, S.; Leitch, B. Synaptic changes in GABAA receptor expression in the thalamus of the stargazer mouse model of absence epilepsy. *Neuroscience* **2015**, *306*, 28–38. [[CrossRef](#)]
30. Seo, S.; Leitch, B. Postnatal expression of thalamic GABAA receptor subunits in the stargazer mouse model of absence epilepsy. *Neuroreport* **2017**, *28*, 1255–1260. [[CrossRef](#)]
31. Farrant, M.; Nusser, Z. Variations on an inhibitory theme: Phasic and tonic activation of GABA(A) receptors. *Nat. Rev. Neurosci.* **2005**, *6*, 215–229. [[CrossRef](#)] [[PubMed](#)]
32. Crunelli, V.; Leresche, N.; Cope, D.W. GABA-A Receptor Function in Typical Absence Seizures. In *Jasper's Basic Mechanisms of the Epilepsies*, 4th ed.; Noebels, J.L., Avoli, M., Rogawski, M.A., Olsen, R.W., Delgado-Escueta, A.V., Eds.; National Center for Biotechnology Information (US): Bethesda, MD, USA, 2012.
33. Cope, D.W.; Hughes, S.W.; Crunelli, V. GABAA receptor-mediated tonic inhibition in thalamic neurons. *J. Neurosci.* **2005**, *25*, 11553–11563. [[CrossRef](#)] [[PubMed](#)]
34. Cope, D.W.; Di Giovanni, G.; Fyson, S.J.; Orban, G.; Errington, A.C.; Lorincz, M.L.; Gould, T.M.; Carter, D.A.; Crunelli, V. Enhanced tonic GABAA inhibition in typical absence epilepsy. *Nat. Med.* **2009**, *15*, 1392–1398. [[CrossRef](#)] [[PubMed](#)]
35. Meeren, H.K.; Pijn, J.P.; Van Luijckelaar, E.L.; Coenen, A.M.; Lopes da Silva, F.H. Cortical focus drives widespread corticothalamic networks during spontaneous absence seizures in rats. *J. Neurosci.* **2002**, *22*, 1480–1495. [[CrossRef](#)]
36. Polack, P.O.; Guillemain, I.; Hu, E.; Deransart, C.; Depaulis, A.; Charpier, S. Deep layer somatosensory cortical neurons initiate spike-and-wave discharges in a genetic model of absence seizures. *J. Neurosci.* **2007**, *27*, 6590–6599. [[CrossRef](#)]
37. McCafferty, C.; David, F.; Venzi, M.; Lorincz, M.L.; Delicata, F.; Atherton, Z.; Recchia, G.; Orban, G.; Lambert, R.C.; Di Giovanni, G.; et al. Cortical drive and thalamic feed-forward inhibition control thalamic output synchrony during absence seizures. *Nat. Neurosci.* **2018**, *21*, 744–756. [[CrossRef](#)]
38. Polack, P.O.; Mahon, S.; Chavez, M.; Charpier, S. Inactivation of the Somatosensory Cortex Prevents Paroxysmal Oscillations in Cortical and Related Thalamic Neurons in a Genetic Model of Absence Epilepsy. *Cereb. Cortex* **2009**, *19*, 2078–2091. [[CrossRef](#)]
39. Pirker, S.; Schwarzer, C.; Wieselthaler, A.; Sieghart, W.; Sperk, G. GABA(A) receptors: Immunocytochemical distribution of 13 subunits in the adult rat brain. *Neuroscience* **2000**, *101*, 815–850. [[CrossRef](#)]
40. Sieghart, W.; Sperk, G. Subunit composition, distribution and function of GABA(A) receptor subtypes. *Curr. Top. Med. Chem.* **2002**, *2*, 795–816. [[CrossRef](#)]
41. Whiting, P.J. GABA-A receptor subtypes in the brain: A paradigm for CNS drug discovery? *Drug Discov. Today* **2003**, *8*, 445–450. [[CrossRef](#)]
42. Mohler, H. GABA(A) receptor diversity and pharmacology. *Cell Tissue Res.* **2006**, *326*, 505–516. [[CrossRef](#)] [[PubMed](#)]
43. Rudolph, U.; Mohler, H. GABA-based therapeutic approaches: GABAA receptor subtype functions. *Curr. Opin. Pharmacol.* **2006**, *6*, 18–23. [[CrossRef](#)] [[PubMed](#)]
44. Nutt, D. GABA(A) Receptors: Subtypes, Regional Distribution, and Function. *J. Clin. Sleep Med.* **2006**, *2*, S7–S11. [[CrossRef](#)] [[PubMed](#)]
45. Packer, A.M.; Yuste, R. Dense, unspecific connectivity of neocortical parvalbumin-positive interneurons: A canonical microcircuit for inhibition? *J. Neurosci.* **2011**, *31*, 13260–13271. [[CrossRef](#)] [[PubMed](#)]
46. Kralic, J.E.; Korpi, E.R.; O'Buckley, T.K.; Homanics, G.E.; Morrow, A.L. Molecular and pharmacological characterization of GABA(A) receptor alpha1 subunit knockout mice. *J. Pharmacol. Exp. Ther.* **2002**, *302*, 1037–1045. [[CrossRef](#)] [[PubMed](#)]
47. McCafferty, C.; Celli, R.; Ngomba, R.T.; Nicoletti, F.; Crunelli, V. Genetic rescue of absence seizures. *CNS Neurosci. Ther.* **2018**, *24*, 745–758. [[CrossRef](#)] [[PubMed](#)]
48. Fremeau, R.T., Jr.; Voglmaier, S.; Seal, R.P.; Edwards, R.H. VGLUTs define subsets of excitatory neurons and suggest novel roles for glutamate. *Trends Neurosci.* **2004**, *27*, 98–103. [[CrossRef](#)]
49. Benarroch, E.E. Glutamate transporters: Diversity, function, and involvement in neurologic disease. *Neurology* **2010**, *74*, 259–264. [[CrossRef](#)]
50. Coleman, J.E.; Nahmani, M.; Gavornik, J.P.; Haslinger, R.; Heynen, A.J.; Erisir, A.; Bear, M.F. Rapid Structural Remodeling of Thalamocortical Synapses Parallels Experience-Dependent Functional Plasticity in Mouse Primary Visual Cortex. *J. Neurosci.* **2010**, *30*, 9670–9682. [[CrossRef](#)] [[PubMed](#)]
51. Nahmani, M.; Erisir, A. VGluT2 immunocytochemistry identifies thalamocortical terminals in layer 4 of adult and developing visual cortex. *J. Comp. Neurol.* **2005**, *484*, 458–473. [[CrossRef](#)]
52. Beneyto, M.; Abbott, A.; Hashimoto, T.; Lewis, D.A. Lamina-specific alterations in cortical GABA(A) receptor subunit expression in schizophrenia. *Cereb. Cortex* **2011**, *21*, 999–1011. [[CrossRef](#)] [[PubMed](#)]
53. Fishell, G. Perspectives on the developmental origins of cortical interneuron diversity. *Novartis Found. Symp.* **2007**, *288*, 21–35, discussion 35–44, 96–108. [[PubMed](#)]
54. Tamamaki, N.; Yanagawa, Y.; Tomioka, R.; Miyazaki, J.; Obata, K.; Kaneko, T. Green fluorescent protein expression and colocalization with calretinin, parvalbumin, and somatostatin in the GAD67-GFP knock-in mouse. *J. Comp. Neurol.* **2003**, *467*, 60–79. [[CrossRef](#)] [[PubMed](#)]
55. Xu, X.; Roby, K.D.; Callaway, E.M. Immunocytochemical characterization of inhibitory mouse cortical neurons: Three chemically distinct classes of inhibitory cells. *J. Comp. Neurol.* **2010**, *518*, 389–404. [[CrossRef](#)]

56. Baude, A.; Bleasdale, C.; Dalezios, Y.; Somogyi, P.; Klausberger, T. Immunoreactivity for the GABAA receptor alpha1 subunit, somatostatin and Connexin36 distinguishes axoaxonic, basket, and bistratified interneurons of the rat hippocampus. *Cereb. Cortex* **2007**, *17*, 2094–2107. [[CrossRef](#)]
57. Martenson, J.S.; Yamasaki, T.; Chaudhury, N.H.; Albrecht, D.; Tomita, S. Assembly rules for GABAA receptor complexes in the brain. *Elife* **2017**, *6*. [[CrossRef](#)]
58. Baur, R.; Minier, F.; Sigel, E. A GABA(A) receptor of defined subunit composition and positioning: Concatenation of five subunits. *FEBS Lett.* **2006**, *580*, 1616–1620. [[CrossRef](#)]
59. Beesley, P.W.; Mummery, R.; Tibaldi, J. N-cadherin is a major glycoprotein component of isolated rat forebrain postsynaptic densities. *J. Neurochem.* **1995**, *64*, 2288–2294. [[CrossRef](#)]
60. Petersen, J.D.; Chen, X.B.; Vinade, L.; Dosemeci, A.; Lisman, J.E.; Reese, T.S. Distribution of postsynaptic density (PSD)-95 and Ca<sup>2+</sup>/calmodulin-dependent protein kinase II at the PSD. *J. Neurosci.* **2003**, *23*, 11270–11278. [[CrossRef](#)]
61. Heller, E.A.; Zhang, W.; Selimi, F.; Earnheart, J.C.; Ślimak, M.A.; Santos-Torres, J.; Ibañez-Tallon, I.; Aoki, C.; Chait, B.T.; Heintz, N. The biochemical anatomy of cortical inhibitory synapses. *PLoS ONE* **2012**, *7*, e39572. [[CrossRef](#)]
62. Tomita, S.; Chen, L.; Kawasaki, Y.; Petralia, R.S.; Wenthold, R.J.; Nicoll, R.A.; Bredt, D.S. Functional studies and distribution define a family of transmembrane AMPA receptor regulatory proteins. *J. Cell Biol.* **2003**, *161*, 805–816. [[CrossRef](#)] [[PubMed](#)]
63. Barad, Z.; Grattan, D.R.; Leitch, B. NMDA Receptor Expression in the Thalamus of the Stargazer Model of Absence Epilepsy. *Sci. Rep.* **2017**, *7*, 42926. [[CrossRef](#)] [[PubMed](#)]
64. Schubert, V.; Dotti, C.G. Transmitting on actin: Synaptic control of dendritic architecture. *J. Cell Sci.* **2007**, *120*, 205–212. [[CrossRef](#)] [[PubMed](#)]
65. Inan, M.; Blazquez-Llorca, L.; Merchan-Perez, A.; Anderson, S.A.; DeFelipe, J.; Yuste, R. Dense and overlapping innervation of pyramidal neurons by chandelier cells. *J. Neurosci.* **2013**, *33*, 1907–1914. [[CrossRef](#)]
66. Galarreta, M.; Hestrin, S. Electrical and chemical synapses among parvalbumin fast-spiking GABAergic interneurons in adult mouse neocortex. *Proc. Natl. Acad. Sci. USA* **2002**, *99*, 12438–12443. [[CrossRef](#)]
67. Harris, K.M.; Weinberg, R.J. Ultrastructure of synapses in the mammalian brain. *Cold Spring Harb. Perspect. Biol.* **2012**, *4*. [[CrossRef](#)]
68. Milenkovic, I.; Vasiljevic, M.; Maurer, D.; Hoger, H.; Klausberger, T.; Sieghart, W. The parvalbumin-positive interneurons in the mouse dentate gyrus express GABA(A) receptor subunits alpha1, beta2, and delta along their extrasynaptic cell membrane. *Neuroscience* **2013**, *254*, 80–96. [[CrossRef](#)]
69. Jafarian, M.; Modarres Mousavi, S.M.; Rahimi, S.; Ghaderi Pakdel, F.; Lotfinia, A.A.; Lotfinia, M.; Gorji, A. The effect of GABAergic neurotransmission on the seizure-related activity of the laterodorsal thalamic nuclei and the somatosensory cortex in a genetic model of absence epilepsy. *Brain Res.* **2021**, *1757*, 147304. [[CrossRef](#)]
70. D'Antuono, M.; Inaba, Y.; Biagini, G.; D'Arcangelo, G.; Tancredi, V.; Avoli, M. Synaptic hyperexcitability of deep layer neocortical cells in a genetic model of absence seizures. *Genes Brain Behav.* **2006**, *5*, 73–84. [[CrossRef](#)]
71. Pisu, M.G.; Mostallino, M.C.; Dore, R.; Mura, M.L.; Maciocco, E.; Russo, E.; De Sarro, G.; Serra, M. Neuroactive steroids and GABAA receptor plasticity in the brain of the WAG/Rij rat, a model of absence epilepsy. *J. Neurochem.* **2008**, *106*, 2502–2514. [[CrossRef](#)]
72. Klausberger, T.; Roberts, J.D.; Somogyi, P. Cell type- and input-specific differences in the number and subtypes of synaptic GABA(A) receptors in the hippocampus. *J. Neurosci.* **2002**, *22*, 2513–2521. [[CrossRef](#)] [[PubMed](#)]
73. Glausier, J.R.; Lewis, D.A. Selective pyramidal cell reduction of GABA(A) receptor alpha1 subunit messenger RNA expression in schizophrenia. *Neuropsychopharmacology* **2011**, *36*, 2103–2110. [[CrossRef](#)] [[PubMed](#)]
74. Bartley, A.F.; Huang, Z.J.; Huber, K.M.; Gibson, J.R. Differential activity-dependent, homeostatic plasticity of two neocortical inhibitory circuits. *J. Neurophysiol.* **2008**, *100*, 1983–1994. [[CrossRef](#)] [[PubMed](#)]
75. Mele, M.; Costa, R.O.; Duarte, C.B. Alterations in GABA(A)-Receptor Trafficking and Synaptic Dysfunction in Brain Disorders. *Front. Cell. Neurosci.* **2019**, *13*, 77. [[CrossRef](#)] [[PubMed](#)]
76. Papp, P.; Kovács, Z.; Szocsics, P.; Juhász, G.; Maglóczy, Z. Alterations in hippocampal and cortical densities of functionally different interneurons in rat models of absence epilepsy. *Epilepsy Res.* **2018**, *145*, 40–50. [[CrossRef](#)] [[PubMed](#)]
77. Studer, F.; Laghouati, E.; Jarre, G.; David, O.; Pouyatos, B.; Depaulis, A. Sensory coding is impaired in rat absence epilepsy. *J. Physiol.* **2019**, *597*, 951–966. [[CrossRef](#)]
78. Richardson, C.A.; Leitch, B. Cerebellar Golgi, Purkinje, and basket cells have reduced gamma-aminobutyric acid immunoreactivity in stargazer mutant mice. *J. Comp. Neurol.* **2002**, *453*, 85–99. [[CrossRef](#)]
79. Leroy, C.; Poisbeau, P.; Keller, A.F.; Nehlig, A. Pharmacological plasticity of GABA(A) receptors at dentate gyrus synapses in a rat model of temporal lobe epilepsy. *J. Physiol.* **2004**, *557*, 473–487. [[CrossRef](#)]
80. Leitch, B. The Impact of Glutamatergic Synapse Dysfunction in the Corticothalamocortical Network on Absence Seizure Generation. *Front. Mol. Neurosci.* **2022**, *15*, 836255. [[CrossRef](#)]
81. Lacey, C.J.; Bryant, A.; Brill, J.; Huguenard, J.R. Enhanced NMDA receptor-dependent thalamic excitation and network oscillations in stargazer mice. *J. Neurosci.* **2012**, *32*, 11067–11081. [[CrossRef](#)]
82. Yao, L.; Grand, T.; Hanson, J.E.; Paoletti, P.; Zhou, Q. Higher ambient synaptic glutamate at inhibitory versus excitatory neurons differentially impacts NMDA receptor activity. *Nat. Commun.* **2018**, *9*, 4000. [[CrossRef](#)] [[PubMed](#)]

83. Fuentealba, P.; Steriade, M. The reticular nucleus revisited: Intrinsic and network properties of a thalamic pacemaker. *Prog. Neurobiol.* **2005**, *75*, 125–141. [[CrossRef](#)] [[PubMed](#)]
84. Wang, Z.; Duan, L. The combined effects of the thalamic feed-forward inhibition and feed-back inhibition in controlling absence seizures. *Nonlinear Dyn.* **2022**, *108*, 191–205. [[CrossRef](#)]
85. Princivalle, A.P.; Richards, D.A.; Duncan, J.S.; Spreafico, R.; Bowery, N.G. Modification of GABA(B1) and GABA(B2) receptor subunits in the somatosensory cerebral cortex and thalamus of rats with absence seizures (GAERS). *Epilepsy Res.* **2003**, *55*, 39–51. [[CrossRef](#)] [[PubMed](#)]
86. Powell, K.L.; Kyi, M.; Reid, C.A.; Paradiso, L.; D'Abaco, G.M.; Kaye, A.H.; Foote, S.J.; O'Brien, T.J. Genetic absence epilepsy rats from Strasbourg have increased corticothalamic expression of stargazin. *Neurobiol. Dis.* **2008**, *31*, 261–265. [[CrossRef](#)] [[PubMed](#)]
87. Kennard, J.T.; Barmanray, R.; Sampurno, S.; Ozturk, E.; Reid, C.A.; Paradiso, L.; D'Abaco, G.M.; Kaye, A.H.; Foote, S.J.; O'Brien, T.J.; et al. Stargazin and AMPA receptor membrane expression is increased in the somatosensory cortex of Genetic Absence Epilepsy Rats from Strasbourg. *Neurobiol. Dis.* **2011**, *42*, 48–54. [[CrossRef](#)]
88. Pfeffer, C.K.; Xue, M.; He, M.; Huang, Z.J.; Scanziani, M. Inhibition of inhibition in visual cortex: The logic of connections between molecularly distinct interneurons. *Nat. Neurosci.* **2013**, *16*, 1068–1076. [[CrossRef](#)] [[PubMed](#)]
89. Xu, H.; Jeong, H.Y.; Tremblay, R.; Rudy, B. Neocortical somatostatin-expressing GABAergic interneurons disinhibit the thalamorecipient layer 4. *Neuron* **2013**, *77*, 155–167. [[CrossRef](#)]
90. Jarre, G.; Altwegg-Boussac, T.; Williams, M.S.; Studer, F.; Chipaux, M.; David, O.; Charpier, S.; Depaulis, A.; Mahon, S.; Guillemain, I. Building Up Absence Seizures in the Somatosensory Cortex: From Network to Cellular Epileptogenic Processes. *Cereb. Cortex* **2017**, *27*, 4607–4623. [[CrossRef](#)]
91. Adotevi, N.; Su, A.; Peiris, D.; Hassan, M.; Leitch, B. Altered Neurotransmitter Expression in the Corticothalamocortical Network of an Absence Epilepsy Model with impaired Feedforward Inhibition. *Neuroscience* **2021**, *467*, 73–80. [[CrossRef](#)]
92. Panthi, S.; Lyons, N.M.A.; Leitch, B. Impact of Dysfunctional Feed-Forward Inhibition on Glutamate Decarboxylase Isoforms and  $\gamma$ -Aminobutyric Acid Transporters. *Int. J. Mol. Sci.* **2021**, *22*, 7740. [[CrossRef](#)] [[PubMed](#)]
93. Jin, H.; Wu, H.; Osterhaus, G.; Wei, J.; Davis, K.; Sha, D.; Floor, E.; Hsu, C.C.; Kopke, R.D.; Wu, J.Y. Demonstration of functional coupling between gamma -aminobutyric acid (GABA) synthesis and vesicular GABA transport into synaptic vesicles. *Proc. Natl. Acad. Sci. USA* **2003**, *100*, 4293–4298. [[CrossRef](#)] [[PubMed](#)]
94. Patel, A.B.; de Graaf, R.A.; Martin, D.L.; Battaglioli, G.; Behar, K.L. Evidence that GAD(65) mediates increased GABA synthesis during intense neuronal activity in vivo. *J. Neurochem.* **2006**, *97*, 385–396. [[CrossRef](#)] [[PubMed](#)]
95. Elmariah, S.B.; Crumling, M.A.; Parsons, T.D.; Balice-Gordon, R.J. Postsynaptic TrkB-mediated signaling modulates excitatory and inhibitory neurotransmitter receptor clustering at hippocampal synapses. *J. Neurosci.* **2004**, *24*, 2380–2393. [[CrossRef](#)] [[PubMed](#)]
96. Maljevic, S.; Krampfl, K.; Cobilanschi, J.; Tilgen, N.; Beyer, S.; Weber, Y.G.; Schlesinger, F.; Ursu, D.; Melzer, W.; Cossette, P.; et al. A mutation in the GABA(A) receptor alpha(1)-subunit is associated with absence epilepsy. *Ann. Neurol.* **2006**, *59*, 983–987. [[CrossRef](#)]
97. Kodera, H.; Ohba, C.; Kato, M.; Maeda, T.; Araki, K.; Tajima, D.; Matsuo, M.; Hino-Fukuyo, N.; Kohashi, K.; Ishiyama, A.; et al. De novo GABRA1 mutations in Ohtahara and West syndromes. *Epilepsia* **2016**, *57*, 566–573. [[CrossRef](#)]
98. Owens, D.F.; Kriegstein, A.R. Is there more to GABA than synaptic inhibition? *Nat. Rev. Neurosci.* **2002**, *3*, 715–727. [[CrossRef](#)]
99. Paxinos, G.; Franklin, K.B. *Paxinos and Franklin's the Mouse Brain in Stereotaxic Coordinates*; Academic Press: Cambridge, MA, USA, 2019.
100. Owe, S.G.; Erisir, A.; Heggelund, P. Terminals of the major thalamic input to visual cortex are devoid of synapsin proteins. *Neuroscience* **2013**, *243*, 115–125. [[CrossRef](#)]